Final Technical Report

UPDATE OF GROUNDWATER AVAILABILITY MODEL FOR BARTON SPRINGS SEGMENT OF THE EDWARDS AQUIFER UTILIZING THE MODFLOW–DCM CODE

SwRI Project 20-14074

Prepared for

Barton Springs Edwards Aquifer Conservation District
and
Texas Water Development Board

April 2009

SOUTHWEST RESEARCH INSTITUTE®
SAN ANTONIO, TEXAS

Final Technical Report

UPDATE OF GROUNDWATER AVAILABILITY MODEL FOR BARTON SPRINGS SEGMENT OF THE EDWARDS AQUIFER UTILIZING MODFLOW–DCM CODE

SwRI Project 20-14074

Prepared for

Barton Springs Edwards Aquifer Conservation District
and
Texas Water Development Board

Prepared by

James R. Winterle
Scott L. Painter
Ronald T. Green

Geosciences and Engineering Division
Southwest Research Institute®
6220 Culebra Road
San Antonio, Texas 78238-5166

April 2009

Table of Contents

List of Figures

List of Tables

Executive Summary

This report documents a modeling study to update the Groundwater Availability Model for the Barton Springs Segment of the Edwards (Balcones Fault Zone) Aquifer to utilize MODFLOW–DCM Version 2.0 (Painter and others, 2007) to explicitly represent conduit flow within the karst aquifer system. This work builds on the Groundwater Availability Model originally developed and documented by Scanlon and others (2001).

The model updates include extending the active model domain to the south and west and definition of a conduit network within the body of the aquifer. These updates necessitated recalibration for steady-state and transient conditions. The steady-state model was calibrated to match observations of hydraulic heads in 74 wells made during July and August 1999 using an estimated average spring discharge of 55 cfs and total pumpage of 5 cfs. The transient model was calibrated to qualitatively match spring discharge measurements at Barton Springs and hydraulic head responses in 3 observation wells for the 10-year period from January 1989 to December 1998. In addition to the model updates and calibrations, a simple algorithm was developed for estimating recharge input to the model based on average monthly precipitation over the recharge and contributing zones.

The root-mean-square residual error for the updated steady-state model is reduced to approximately half that of the original Groundwater Availability Model. The transient model was able to reproduce the pattern of hydraulic head fluctuations in observation wells, and observed discharge at Barton Springs using recharge input that was developed from the precipitation-to-recharge algorithm. The calibrated transient model performed well in matching the springflow conditions and the cumulative spring flow for the 10-year simulation period.

Development of a more complex precipitation-to-recharge algorithm is recommended to account for a portion of recharge that can be delayed by slow drainage from the vadose zone. The added complexity, if pursued, would permit improved understanding of the importance of vadose zone storage and delayed recharge to management of the aquifer resources.

1 Introduction

This report documents a modeling study to update the Groundwater Availability Model for the Barton Springs Segment of the Edwards (Balcones Fault Zone) Aquifer to utilize MODFLOW–DCM Version 2.0 (Painter and others, 2007) to explicitly represent conduit flow within the karst aquifer system. This work builds on the Groundwater Availability Model originally developed and documented by Scanlon and others (2001), which is referenced extensively throughout this report. The underlying conceptual and geologic frameworks of the original Groundwater Availability Model remain essentially unchanged. Building upon this excellent foundation, this study documents the following updates to the original modeling approach:

- Implementation of MODFLOW–DCM through addition of a separate interacting model domain that represents a network of high-permeability conduits nested within the main aquifer layer

- Extension of the active model area to the south and west

- Initial development of an approach for deriving recharge input to the model based on monthly average precipitation data.

These updates necessitated recalibration of the model and sensitivity analyses to evaluate model performance in terms of its ability to predict well water-level elevations and discharge from Barton Springs. The calibration and sensitivity analyses results are documented in this report in a manner intended to meet the Texas Water Development Board's format and content requirements for Groundwater Availability Models.

2 Study Area Physiography, Geology, and Climate

Key features of the study area are summarized in this section. Additional descriptions of the physiography, geology, and climate of the study area can be found in Scanlon and others (2001).

The Edwards (Balcones Fault Zone) Aquifer is physiographically located at the transition between the Edwards Plateau to the northwest and the Blackland Prairie to the southeast. In general, the Edwards (Balcones Fault Zone) Aquifer is structurally controlled by the relative uplift of the Edwards Plateau along the Balcones Fault Zone. This faulting has developed three zones associated with the Edwards (Balcones Fault Zone) Aquifer: the contributing zone, the recharge zone, and the confined zone (Figure 1). Normal faulting along *en echelon* faults and grabens associated with the uplift of the Edwards Plateau have resulted in exposure of the underlying Glen Rose Formation to the north and northwest of the Edwards (Balcones Fault Zone) Aquifer. This region is referred to as the contributing zone to the Edwards (Balcones Fault Zone) Aquifer. Continued faulting to the south and southeast has exposed the Edwards Group at the surface. This region is referred to as the recharge zone. Farther to the south and southeast, younger, less permeable units overlay the Edwards (Balcones Fault Zone) Aquifer, causing the aquifer

to be confined. The southern and southeastern extent of the Edwards Group is defined by the transition from fresh to saline water, commonly designated as water with total dissolved solids in excess of 1,000 ppm.

The Edwards (Balcones Fault Zone) Aquifer is geographically divided into three subsections: the Southern or San Antonio segment, the Barton Springs segment, and the Northern segment. The Barton Springs segment is located in Hayes and Travis Counties (Figure 1). The Barton Springs segment is terminated by a groundwater divide near Buda on the west and the Colorado River to the east.

The Barton Springs segment, including the contributing zone, is approximately 25 mi long and 12.5 mi wide. The recharge zone of the Barton Springs segment covers 100 mi^2. Along this segment, the Edwards (Balcones Fault Zone) Aquifer has an approximate thickness of 100–600 ft, with thickness greatest on the down-dip side. Most fault orientations are coincident with the Balcones Fault Zone orientation, which tends to be northeast-southwest in the Barton Springs segment. Also oriented coincident with the Balcones Fault Zone orientation are the main groundwater karst conduits whose location and orientation have been inferred using results from tracer tests as shown in Figure 2 (Hauwert and others, 2002; Hunt and others, 2006).

The study area is in a subtropical humid climate zone. Annual precipitation ranged from 11 to 65 inches per year during the period from the years 1860 to 2000, based on records from weather stations located at Camp Mabry and Mueller Airport in Austin. The mean annual precipitation for this period is 33.5 inches, with a majority of precipitation resulting from frontal systems during the spring and fall. Convectional thunderstorms during the summer result in a smaller fraction of total precipitation but can be locally heavy.

3 Previous Work

Scanlon and others (2001) developed the original Groundwater Availability Model for the Barton Springs segment of the Edwards (Balcones Fault Zone) Aquifer using MODFLOW–96 (Harbaugh and McDonald, 1996), a modular finite-difference code developed by the U.S. Geological Survey to model groundwater flow. The model was calibrated for steady-state conditions using a recharge rate based on the average spring discharge of 55 cfs plus pumpage for 1989 of 5 cfs. The model was calibrated to transient conditions for the ten-year period from 1989 to 1998. This model generally reproduced spring flow observations for the transient period. However, simulated spring flows during high-flow periods tended to be larger than observed and simulated water-level hydrographs for observation wells fluctuated more strongly to changes in recharge than the observed hydrographs. Additionally, simulated heads in the southwest portion of the model tended to be too high. Additionally, simulated spring flows for extreme drought conditions tended to be lower than observed. To address this problem, Barton Springs Edwards Aquifer Conservation District developed an alternative calibration of the model for simulating extreme low-flow conditions (Smith and Hunt, 2004).

As part of a long-term project to develop new modeling approaches and tools to address applications involving karst aquifers with significant conduit flow, Southwest Research Institute® (SwRI) developed MODFLOW–DCM Version 2.0 and used it to model the Barton Springs Segment (Painter and others, 2007). The MODFLOW–DCM code adopts a dual-continuum approach to explicitly model a discrete conduit flow system domain nested within and able to exchange mass with a diffuse flow system. Attributes of MODFLOW-DCM include the ability to transition between turbulent and laminar flow within the conduit system whenever the hydraulic gradient exceeds a specified critical gradient. The code also contains enhancements to solve numerical convergence problems with the original MODFLOW–2000 software using a new algorithm for simulating the rewetting of dry cells when water levels fluctuated above and below cell elevations.

Painter and others (2007) used the Scanlon and others (2001) model as a starting point and added a separate numerical layer to represent conduits using the MODFLOW–DCM code. The model was calibrated to hydraulic head and spring flows for steady and transient conditions and successfully simulated the drying and rewetting of cells in the unconfined recharge zone. In addition, sensitivity analysis indicated that the addition of the turbulence model resulted in an improved match to the dynamic spring hydrograph for Barton Springs and that the matrix/conduit exchange parameter can be adjusted to allow for a better match of dynamic spring flow. Model results also highlighted a moderate sensitivity of spring discharge to conduit elevation relative to matrix elevation. The MODFLOW–DCM simulation of drought conditions better matched hydraulic head and spring discharge than the original Groundwater Availability Model.

The model update described in this report is a continuation of the work of Painter and others (2007), with the intention to meet the Texas Water Development Board requirements for use as a Groundwater Availability Model for the Barton Springs Segment of the Edwards (Balcones Fault Zone) Aquifer.

4 Hydrogeologic Setting

4.1 Hydrostratigraphy

The hydrostratigraphy considered in this study is the same as that developed by Scanlon and others (2001). Layer elevations for aquifer top and bottom were used directly without modification. One key difference, however, is the explicit inclusion of a conduit flow system within the aquifer layer. Painter and others (2007) set the top of the conduit system to coincide with the top of the Kirshberg member throughout most of the model and 50 ft below the top of the Kirshberg member of the Edwards Group in the recharge zone in Hayes County. Additional adjustments to conduit elevations by Painter and others (2007) were made based on numerical experiments and discussions with Barton Springs Edwards Aquifer Conservation District staff. Conduit system properties are discussed further in Section 6.3.

4.2 Structure

The underlying conceptual model for geologic structure in the model is unchanged from the original Groundwater Availability Model of Scanlon and others (2001). The geologic structure is carried forward to the model in terms of top and bottom layer elevations for the main aquifer layer, referred to as the diffuse system in this study. Fault zones within the aquifer system can have the effect of acting as a barrier to flow across the fault and may facilitate flow along the direction of the fault strike. These effects were incorporated by Scanlon and others using the MODFLOW Horizontal Flow Barrier (HFB) package to assign three zones to represent reduced permeability across fault zones (Figure 3). The properties assigned to the MODFLOW HFB package for this study are unchanged from the original Groundwater Availability Model.

4.3 Water Levels and Regional Groundwater Flow

The underlying conceptual model for water levels and regional groundwater flow is unchanged from the original Groundwater Availability Model of Scanlon and others (2001). Observations indicate that water levels in wells can vary as much as 90 ft in response to recharge events. The transient model calibration attempts to match this variability. Regional groundwater flow into and out of the system is not believed to be significant.

4.4 Recharge

The underlying conceptual model and basis for recharge locations are essentially unchanged from the original Groundwater Availability Model by Scanlon and others (2001). Eighty-five percent of the recharge is assumed to be focused along six creeks (i.e., Barton, Williamson, Slaughter, Bear, Little Bear, and Onion) and the remaining 15 percent of recharge is assumed to be distributed uniformly across the recharge zone. This assumed distribution of focused and distributed recharge was carried forward from an earlier model by Slade and others (1985).

4.5 Rivers, Streams, Springs

The assessment of rivers, streams, and springs in the model area as presented by Scanlon and others (2001) is adopted in its entirety in this study. Five major drainage basins in the model area contain the catchment areas for Barton, Williamson, Slaughter, Bear, Little Bear, and Onion creeks where focused recharge occurs. Most of the flow in the aquifer that is not pumped by wells eventually discharges to Barton Spring and a lesser amount is discharged from nearby Cold Springs (see Figure 1).

4.6 Hydraulic Properties

An assessment of hydrologic properties in the model area is provided by Scanlon and others (2001). Aquifer transmissivity values estimated from aquifer tests span several orders of magnitude and generally are not useful for estimating zonal properties for the

flow model because of the difference in the scale represented by the test data. In this model update, the conceptual model for hydraulic properties is modified to a dual-permeability concept. The dual-permeability concept in this case refers to the interaction of a relatively low-permeability diffuse flow system that occupies most of the aquifer volume with a conduit flow system that occupies only a small fraction of the aquifer volume, but is capable of conducting a substantial portion of total water movement in the system. Hydraulic conductivities and storage properties of the diffuse and conduit flow systems are discussed further in Sections 8 and 9.

4.7 Discharge

The assessment of discharge in the model area provided by Scanlon and others (2001) is adopted in this study. Most of the flow in the aquifer discharges to Barton Spring, with a lesser amount discharged at Cold Springs. Reliable discharge measurements are only available for Barton Springs. Discharge from Cold Springs occurs through a series of diffuse seeps that cannot be reliably measured, but the volume is generally assumed to be approximately 6 percent of the total spring discharge based on results of the current Groundwater Availability Model by Scanlon and others (2001).

4.8 Water Quality

An assessment of water quality in the model area is provided by Scanlon and others (2001). This study makes no attempt to evaluate water quality within the flow system.

5 Conceptual Model of Groundwater Flow in the Aquifer

The conceptual model for groundwater flow in the aquifer is modified somewhat from that of Scanlon and others (2001). Here, the aquifer is conceptualized as having two interacting flow systems. A diffuse flow system of relatively low permeability occupies the bulk of the aquifer volume and therefore accounts for nearly all of the storage capacity. Flow in the diffuse system is described by Darcy's Law where the flow rate is proportional to the hydraulic conductivity and hydraulic gradient. The conduit flow system is conceptualized as a network of interconnected conduits within the diffuse flow system. Although the conduit system occupies a tiny fraction of the total aquifer volume, it facilitates a large fraction of the total water movement between recharge and discharge locations. For example, less than 1 percent of model cells are assigned as conduits but 85 percent of recharge is assigned directly into the conduit system and all spring discharge exits through the conduit system.

The majority (85%) of the recharge is assigned to the focused recharge locations, consistent with assessments by Puente (1976, 1978). The focused recharge locations, shown in Figure 4, all coincide with conduits that can rapidly distribute water through the aquifer system. The remainder of recharge (15%) is assumed to be distributed uniformly to the recharge zone where the Edwards formation is present in outcrop (green shaded area in Figure 4). The assumption that focused recharge enters directly into conduits, rather than distributed along entire stream channels, was carried forward from the model

of Painter and others (2007) and reflects a conceptual model that, as streams flow across the outcrop zone, they lose substantial amounts of water through infiltration into highly permeable faults or fracture zones, which are represented in the model by the conduit system. Indeed, as shown in Figure 2, several of the features represented in this model have been identified as highly permeable features and utilized for dye tracer tests (e.g., Hunt and others, 2006).

Focused recharge to the aquifer results from storm water runoff in the contributing zone flowing into one of the five major stream drainages in the study area. In this study, we estimate recharge as a function of average monthly precipitation over the model area. It is assumed that no recharge will occur below a certain precipitation threshold. This threshold represents water taken up by interception storage, residual soil moisture, and plant evapotranspiration. Above this threshold, recharge increases linearly with increasing precipitation until a certain limit, after which recharge feature will not increase further. This limit represents the maximum rate at which the recharge can accept water such that any additional precipitation will run off the recharge zone as streamflow.

All recharge that enters the aquifer eventually discharges to either a pumping well or one of two springs. Discharge to pumping wells represents about 6 percent of the total long-term average discharge and outflow from Cold Springs is also estimated to be approximately 6 percent of average discharge (Scanlon and others, 2001). The remainder of discharge occurs at Barton Springs. The hydraulic nature of the aquifer is dynamic and responds rapidly to recharge events in terms of both spring discharge and well water levels.

The boundary of the updated Groundwater Availability Model is extended to the west and south compared to the boundaries considered by Scanlon and others (2001), as shown in Figure 5. The aquifer is unconfined in the outcrop zone (green shaded area in Figure 5). Farther to the southeast the aquifer is confined by the Del Rio Clay. The surface of the aquifer plunges to the southeast. The southeast boundary of the Edwards (Balcones Fault Zone) Aquifer terminates at the "Bad-Water Line," beyond which the total dissolved solids of the water exceeds 1,000 mg/L and is not suitable for drinking. To the southwest, the model boundary is intended to coincide with the approximate area of a groundwater divide.

6 Model Design

Model design includes information on the code and processor, aquifer discretization, model input parameters, and model boundaries.

6.1 Code and Processor

The model presented in this study utilizes MODFLOW–DCM, a variant of standard MODFLOW developed to accommodate both diffuse and conduit flow (Painter and others, 2007). The model will run on standard desktop personal computers with any of the Microsoft Windows-based operating systems.

Input for MODFLOW–DCM is the same as standard MODFLOW–2000 (Harbaugh and others, 2000), with two exceptions: (1) the standard MODFLOW solver packages are replaced with the NR1 solver package, and (2) the LPF groundwater flow module is replaced with the DCM groundwater flow module. Input file formats and explanation of parameters for the DCM and NR1 modules are provided in Appendix A (reproduced from Painter and others, 2007).

Input to the MODFLOW–DCM variant input file is similar to the LPF package, but has no information relating to vertical flow or rewetting algorithms. Instead, two parameters describing the conduit-diffuse exchange rate and the critical gradient for onset of turbulent flow are required.

The NR1 solver is automatically activated with default parameters if no input file is provided. An NR1 input file with the name *nr1in.dat* that specifies the modified settings should be used if the model solution does not converge properly with the default settings. For this application, an *nr1in.dat* input file was needed to specify an increased number of outer iteration loops for the transient simulations to achieve convergence. Additional details on the workings of the NR1 solver can be found in Painter and others (2008).

It should be noted that MODFLOW–DCM presently is not compatible with most of the pre- and post-processing software commonly used with MODFLOW–2000 (e.g., Groundwater Vistas, Visual MODFLOW, Groundwater Modeling System, etc.). Models developed with those software packages can, however, easily be converted to run with MODFLOW–DCM by modifying the input file for the LPF groundwater flow module using the input instructions provided for the DCM module in Appendix A.

6.2 Layers and Grid

This model utilizes a 120x120 grid system for each of the two numerical layers (diffuse and conduit). However, flow only occurs in the grid cells identified as active. For the diffuse system, the number of active cells is increased compared to the Scanlon and others (2001) model, as shown in Figure 5. This extended model domain is based on input from Barton Springs Edwards Aquifer Conservation District which provided a set of MODFLOW–96 input files with expanded boundaries to the southwest and southeast (Brian Smith, Barton Springs Edwards Aquifer Conservation District, personal communication). The active grid matrix from the *bas.dat* file and layer elevations from the *bcf.dat* file provided by Barton Springs Edwards Aquifer Conservation District were incorporated into the MODFLOW–DCM input files used in this modeling study. The active domain for the conduit system is the same as developed by Painter and others (2007) and is shown in Figure 6.

The grid cells are 1000 ft long and 500 ft wide. The grid is aligned with the predominant northeast strike of faults in the model domain and is thus rotated 45 degrees counterclockwise from the east–west direction. The active model domain for the diffuse system extends from a presumed groundwater divide near Buda, Texas, in the southwest

to the Colorado River near downtown Austin along the northeastern boundary. The southeastern boundary corresponds to the fresh-water/saline-water interface, and the northwestern boundary corresponds to the Mount Bonnell Fault.

6.3 Model Parameters

For each of the two numerical layers (diffuse and conduit), model parameters include (1) elevations of the top and bottom of the layer, (2) horizontal hydraulic conductivity, (3) specific yield (for unconfined conditions), and (4) specific storage (for confined conditions). Specific yield and specific storage are required only for the transient simulations. For the diffuse system only, an additional parameter is the hydraulic characteristic for horizontal flow barriers. For the conduit system only, two new parameters are the rate coefficient for conduit-diffuse exchange and the critical gradient for onset of turbulent flow.

The diffuse system top and bottom elevations used in this model are those developed by Scanlon and others (2001). The top of the aquifer is based on ground-surface elevation in the outcrop zone and the base of the Del Rio Clay in the confined zone. The bottom elevation of the aquifer corresponds to the base of the Walnut Formation as interpreted by Small and others (1996).

The conduit representation in the MODFLOW–DCM model was developed by Painter and others (2007) in collaboration with Barton Springs Edwards Aquifer Conservation District staff. Conduit placement is based on major flow paths inferred from the dye tracer studies of Hauwert and others (2002) and Hunt and others (2006) (Figure 2). In addition, conduits were located so that known locations for focused recharge were intercepted by conduits. The conduit network, which is composed of 13 individual conduits, numbered 2 through 14, is shown in Figure 6. The number 1 is reserved as a zero-permeability zone designator for cells in the conduit grid not occupied by conduits. Conduits 2 and 12 are the main flow paths as they each traverse the entire length of the model domain. Conduit 6 also channels significant flow directly to Barton Springs. Conduit 13 represents a junction point where conduits 2, 6, and 12 arrive at spring discharge locations. With the exception of conduit 7, flow in all other conduits eventually arrives at conduit 13. Hydraulic interactions between conduits can occur wherever they intersect each other.

Although these major conduit locations have been identified with some degree of confidence by the tracer tests, a perhaps irreducible uncertainty is the internal geometry and elevation of each conduit within the aquifer system. The true number of conduits and their internal geometry likely will never be known with a high degree of certainty, but the overall effect of major conduits on the spring discharge and water level response to recharge events can be represented sufficiently by making some reasonable approximations based on available observations and calibrating to match the system response to recharge events.

Conduit thickness was taken as 30 ft based on the initial conduit model calibration by Painter and others (2007). Sensitivity of the model to conduit elevation was examined by Painter and others (2007) and shown to have only a modest effect on the response time of spring flows to changes in recharge conditions. The conduit geometry developed by Painter and others (2007) is used in this study without further modification.

It is important to note that, although the cells occupied by the conduit in this model have dimensions of 1000 ft by 500 ft, these dimensions should not be interpreted to represent the geometry of the conduits. Conduit length and width are not specified but, conceptually, a conduit traverses the length of each cell in the direction that connects one conduit cell to another. The volume of the cell occupied by a conduit could be inferred from the value of the assigned storage parameter if aquifer compressibility and residual water capacity are known. For example, if compressibility and residual water capacity are negligible in an unconfined system, specific yield could be taken as an approximate representation of the fraction of conduit void volume. In this example, if the specified 30-ft conduit thickness represents approximately 10 percent of the saturated thickness in a 500-ft wide cell, then the effective conduit width implied by a specific yield value of 0.0004 (see transient calibration in Section 9) would be about 2 ft. Although the authors do not propose that 2 ft should be taken as a reliable estimate of conduit width, it does suggest a plausible representation of conduits for modeling purposes.

Hydraulic conductivities for the 9 zones of the diffuse system (Figure 7) and the 13 conduits (Figure 6) were estimated during the steady-state calibration as explained in Section 8. Specific yield and specific storage parameter values were estimated during the transient calibration process as explained in Section 9. Using these hydraulic conductivity and storage parameters, the model is set up to calculate transmissivity and storativity on the basis of saturated thickness.

Hydraulic characteristics for horizontal flow barriers in the diffuse system are the same as used in the Groundwater Availability Model by Scanlon and others (2001). The values for hydraulic characteristic represent hydraulic conductivity divided by the width of the horizontal barrier. Horizontal flow barriers are only applied in the diffuse system.

The diffuse system was designated as confined/unconfined, which permits the calculation to switch between confined or unconfined solution algorithms if calculated heads rise above or fall below the layer top elevation. The length unit is feet, and the time unit is days for all input and output.

6.4 Model Boundaries and Initial Conditions

Boundaries and initial conditions were assigned for (1) recharge, (2) well pumping, (3) springs, and (4) starting heads.

For the base case, 85 percent of recharge is assumed to be concentrated along losing streams as shown in Figure 4, and the remaining 15 percent is distributed uniformly across the recharge zone. This apportionment of recharge between diffuse and focused

areas is the same as used by Scanlon and others (2001), based on studies conducted by Barrett and Charbeneau (1996) and consistent with the estimates by Slade and others (1985) and Puente (1976, 1978).

Treatment of well pumping is the same as implemented by Scanlon and others (2001). That is, pumping is assigned to cells on the basis of the location of pumping wells reported to the Barton Springs Edwards Aquifer Conservation District. Scanlon and others estimated unreported domestic (rural) pumpage from countywide estimates to be approximately 5 percent of total pumping and assigned a small value for pumping rate to all active cells to account for the distributed nature of unreported pumping. These same pumping rates are used for both the transient and steady-state calibrations in this study.

Spring flows are accounted for using the Drain Package of MODFLOW to represent Barton Springs and Cold Springs. The drain elevation is the spring elevation (432 ft for Barton Springs and 430 ft for Cold Springs), and a high drain conductance value was used (i.e., 1,000,000 ft^2/d) to allow unrestricted discharge of water. The drain locations are assigned to the conduit system.

The initial head for the steady-state simulations was the top of the aquifer. After calibration was achieved, however, the calibrated heads were saved as the new starting heads, which resulted in faster run times. For transient simulations, the steady-state model was run with a reduced recharge rate to generate a set of starting heads consistent with the ~25 cfs spring discharge rate at the beginning of the transient simulation period. This step was necessary because the steady-state model was calibrated to match a spring discharge rate of 55 cfs, which is about double the observed discharge during the first time step of the transient model. The steady-state model was therefore rerun with the calibrated parameter set and lower recharge rate to obtain a set of initial heads that reflect conditions observed at the beginning of the transient simulation.

All lateral boundaries are assigned no-flow conditions such that no flow enters or leaves the model domain through those boundaries. This treatment of lateral boundaries was carried forward from the Groundwater Availability Model developed by Scanlon and others (2001).

7 Modeling Approach

Beginning with the Barton Springs Segment of the Edwards (Balcones Fault Zone) Aquifer model developed by Painter and others (2007) using MODFLOW–DCM, the active model domain was extended, as previously described, using information provided by Barton Springs Edwards Aquifer Conservation District. The modeling approach taken with this extended-domain model was to (1) calibrate the model to steady-state conditions by varying hydraulic conductivity parameters, (2) develop an algorithm for estimating time-varying recharge input based on monthly average precipitation estimates, and (3) calibrate for a 10-year transient simulation period by varying aquifer storage parameters and recharge algorithm parameters to match spring discharge rates and observed water

levels. The steady-state and transient calibration processes are described in sections 8 and 9, respectively.

The algorithm for estimating recharge from average monthly precipitation represents an initial attempt to utilize the model to estimate recharge rates as a function of precipitation. Previous models by Scanlon and others (2001) and Painter and others (2007) estimated total recharge over the model area using a simple approach of assuming it to be equal to the total of spring discharge plus well pumping. For transient simulations, this approach led to a good match between modeled and observed spring discharge rates. A limitation of this approach, however, is that it cannot be used in a predictive manner to model spring discharge because the recharge input requires *a priori* knowledge of spring discharge. By developing recharge input as a function of precipitation over the model area, the predictive ability of the model is improved because synthetic precipitation records can be generated to evaluate groundwater management options under various scenarios of drought or deluge.

As this study represents an initial attempt to develop a precipitation-to-recharge function, a direct approach is taken. As discussed later under recommendations for future improvements in Section 11, additional studies may wish to explore more complex approaches for this function. Average monthly precipitation estimates for the recharge and contributing zone area were obtained from the City of Austin (Roger Glick, personal communication). Precipitation for each of the contributing zone watersheds is not separately considered.

The recharge algorithm developed for this model assumes that an initial threshold (P_{thresh}) of monthly precipitation (P) must be exceeded before any recharge (R) can occur. Above this threshold, it is assumed recharge will occur in either linear or exponential proportion to the amount of precipitation. A final assumption is that a limit in the amount of precipitation (P_{limit}) exists such that any additional precipitation will leave the recharge area as runoff and the recharge rate will remain constant. Based on these assumptions, the following algorithm is used to estimate monthly recharge from monthly precipitation

$$\begin{aligned} &\text{For } P < P_{thresh} && R = 0 \\ &\text{For } P_{thresh} < P < P_{limit} && R = C \times (P - P_{thresh})^{\lambda} \\ &\text{For } P > P_{limit} && R = P_{limit} \end{aligned}$$

where C is a constant of proportionality and λ describes an exponential relationship between precipitation and recharge. This function can be set to a simple linear proportionality by setting the value of λ to unity. The parameters P_{thresh}, P_{limit}, C and λ are used as fitting parameters during the transient calibration to develop recharge input that provides a reasonable match between simulated and observed spring discharge.

It should be noted that this precipitation-to-recharge algorithm is executed entirely outside of the MODFLOW–DCM model and, as such, is not considered a part of the Groundwater Availability Model update. Thus, future improvements to this algorithm to

further improve the ability to estimate recharge would not be part of recalibration of the model.

8 Steady-State Model

The steady-state model follows an approach similar to that used by Scanlon and others (2001) and Painter and others (2007). The total amount of recharge for the steady-state model is assumed to equal the long-term (1918 through 1999) average spring discharge of 55 cfs for Barton and Cold Springs. Total pumpage was assumed equal to the 1989 average pumping rate of 5 cfs. As previously described, focused recharge is assumed to be 85 percent of total recharge and is distributed according to the proportions indicated in Figure 4. The remaining 15 percent of recharge is distributed among model cells in the recharge zone. An initial *rch6.dat* input file was developed to represent the proportional distribution of recharge shown in Figure 4. A recharge-multiplier parameter, specified in the *rch6.dat* file, was then adjusted to fine tune the total recharge input to obtain a calculated steady-state spring discharge equal the average spring-discharge rate of 55 cfs.

8.1 Calibration

Hydraulic head observations obtained from 74 wells during July and August 1999 were used as calibration targets (Figure 8). This time period was selected by Scanlon and others (2001) to approximately reflect average conditions throughout the model domain. The total range of hydraulic head values represented by these observation wells is 278 ft. Hydraulic conductivity values for the 9 diffusive zones and 13 conduits was varied using a trial-and-error approach to obtain the best match to hydraulic heads at the 74 observation points. The goal of the calibration was to minimize the root-mean-square of the residual error between simulated and observed water levels.

Two alternative calibrated models were developed. For the base case, referred to as Calibration 1, the conduit-diffuse exchange parameter (α_0) is 0.001 per day, as used by Painter and others (2007). For the alternative case, referred to as Calibration 2, α_0 is 0.01 per day. The purpose for developing two alternative calibrations is to support an analysis of the sensitivity of transient simulations to the rate of conduit-diffuse mass exchange, as described in Section 9.2.

Table 1 shows the calibration statistics and residual error plots for Calibrations 1 and 2. The root-mean-square residual errors are 15.9 ft and 16.3 ft, respectively, which is about 6 percent of the total range of observed head. Thus, both calibrations meet the TWDB Groundwater Availability Model criterion of root-mean-square residual error less than 10 percent of the total hydraulic head range. This error is also well within the range of observed temporal fluctuations in hydraulic heads throughout the modeled area. Although, Calibration 2 has a slightly greater root-mean-square error, it has slightly better mean absolute error. The residual error plots in Table 1 show errors for both models are distributed approximately evenly above and below the zero-error line, resulting in a mean error close to zero for both models. Figure 9 shows that positive and negative residual errors for Calibration 1 are uniformly distributed throughout the model, indicating there

is no spatial bias in the calculated hydraulic heads. A similar plot is not shown for Calibration 2 because it is visually indistinguishable from the one shown in Figure 9. Overall, Calibration 1 is preferable only for its somewhat narrower range between minimum and maximum residual errors. Additionally, as will be discussed in Section 9.2, Calibration 1 performs slightly better in terms of matching spring discharge rates in the transient simulations.

8.2 Sensitivity Analysis

Table 2 lists the calibrated hydraulic conductivity values for the two models. In general, the increased rate of conduit-diffuse exchange for Calibration 2 necessitated increases in diffuse zone conductivity and decreases in conduit conductivity to bring the calibration error back to the levels of Calibration 1. The greatest magnitude of difference between calibrated hydraulic conductivities for the two models is for Conduit Zone 12, which is 7 times as great for Calibration 1 compared to Calibration 2.

Table 1. Calibration statistics and residual error plots for base (calibration 1) and alternative (calibration 2) steady-state calibrations.

Statistic	Calibration 1, α_0 = 0.001 per day	Calibration 2, α = 0.01 per day
Root-Mean-Square Error (ft)	15.9	16.3
Mean Absolute Error (ft)	12.8	12.7
Mean Error (ft)	0.008	0.03
Minimum Residual (ft)	-30.5	-38.8
Maximum Residual (ft)	35.2	44.9
Residual Error Plots		
Calibration 1 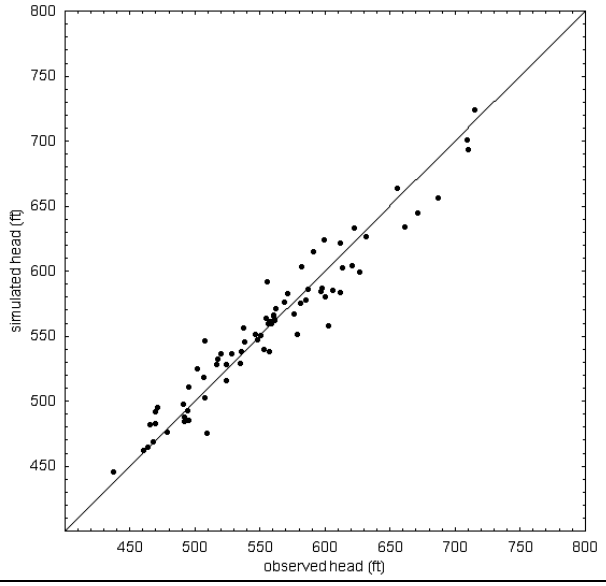		Calibration 2 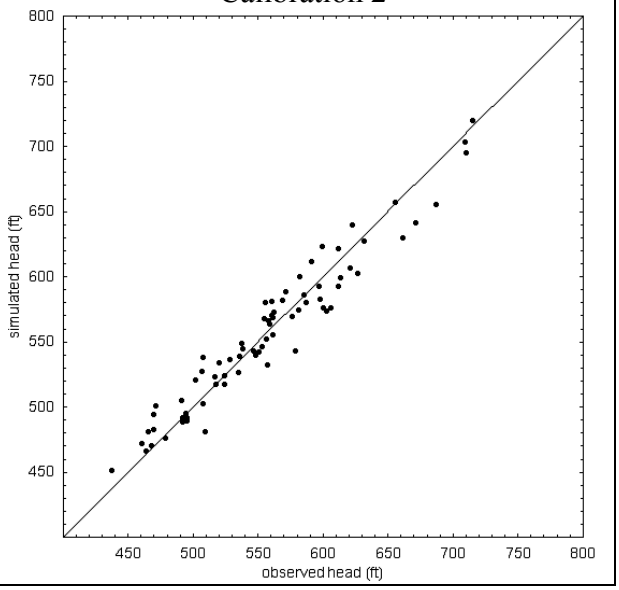

Table 2. Calibrated hydraulic conductivity values for the 9 diffuse-system zones and 13 conduits for Calibration 1 and Calibration 2.

Calibrated Hydraulic Conductivity (ft/d)		
	Calibration 1	**Calibration 2**
Diffuse Zone 1	0.5	0.5
Diffuse Zone 2	15.0	54.0
Diffuse Zone 3	0.4	0.5
Diffuse Zone 4	1.5	1.5
Diffuse Zone 5	2.0	2.0
Diffuse Zone 6	17.0	20.0
Diffuse Zone 7	2.3	3.0
Diffuse Zone 8	10.0	12.0
Diffuse Zone 9	100	150
Conduit Zone 2	160,000	135,000
Conduit Zone 3	22,000	22,000
Conduit Zone 4	12,000	15,000
Conduit Zone 5	10,000	8,000
Conduit Zone 6	40,000	50,000
Conduit Zone 7	20,000	20,000
Conduit Zone 8	5,000	5,000
Conduit Zone 9	3,200	3,000
Conduit Zone 10	6,000	6,000
Conduit Zone 11	1,000	1,000
Conduit Zone 12	4,300	600
Conduit Zone 13	100,000	100,000
Conduit Zone 14	1,000	1,000

During calibration it was evident that the model is particularly sensitive to the hydraulic conductivity of conduits 2 and 12, which is not surprising since both of these conduits traverse most of the length of the model and all other conduits, with the exception of conduit 7, connect to either conduit 2 or 12 or both.

In the case of conduit 2, it was necessary to assign an extremely high hydraulic conductivity value compared to the other conduits. Attempts during the calibration to find parameter combinations that would permit assigning lower conductivity to conduit 2 were not successful. In other words, the model seems to need a high permeability pathway through the center of the model to reproduce the pattern of observed hydraulic heads.

The combination of hydraulic conductivities in conduit 12 and diffuse zone 2 also proved to be important parameters in the calibration process. Both conduit 12 and zone 2 traverse the length of the model in an area south of most of the observation wells. Increasing or decreasing the conductivity of either conduit 12 or zone 2 had essentially the same effect of uniformly decreasing or increasing calculated hydraulic heads at all of the observation well locations. This effect was used during the calibration to keep the mean error close to zero by adjusting these parameter values to keep the residuals distributed evenly above and below the zero-error line. Since either parameter could be adjusted to have the same effect, there is no unique combination of these two parameters that provides a best calibration. Note in Table 2 that, for Calibration 2, diffuse zone 2 conductivity is significantly increased compared to Calibration 1, which necessitated a corresponding significant decrease in the conductivity of conduit 12. Thus, the two calibrated models represent two distinctly different combinations of conduit 12 and zone 2 hydraulic conductivities. As will be shown in Section 9.2, however, the two different calibrations do not substantially affect the results of transient simulations.

9 Transient Model

For the transient simulations, the model solution is divided into 120 monthly stress periods with varying recharge boundary conditions to reflect monthly recharge and well pumping for the 10-year period from 1989 through 1998. The well-pumping rates used in this model are the same as those developed by Scanlon and others (2001). Recharge was estimated using the algorithm described in Section 7 to convert average monthly precipitation into the recharge input for each stress period. Daily precipitation values were summed to obtain the monthly totals used to develop the recharge input for each stress period (Figure 10).

The input parameter set for conduit- and diffuse-system hydraulic conductivities is based on the base case steady-state calibrated model (Calibration 1 in Section 8). Starting heads for the transient simulations were developed by running the steady-state model at a lower recharge rate to obtain starting heads consistent with the observed discharge rate of approximately 25 cfs at Barton Springs at the beginning of the 10-year transient simulation period.

9.1 Calibration

Transient calibration was conducted using a trial-and-error approach for adjusting aquifer storage parameters (specific storage and specific yield) and the precipitation-to-recharge transfer function parameters (P_{thresh}, P_{limit}, C and λ, defined in Section 7) to achieve a best fit to observed discharge at Barton Springs and observed heads in three observation wells for the 10-year simulation period.

Because the ability to predict low spring flows is an important aquifer management objective, a key calibration target was to match the timing and magnitude of low springflow events. Additionally, recharge input was calibrated to obtain a match between the calculated and observed cumulative spring flow for the entire 10-year simulation period. A third calibration target was to obtain a reasonable match between calculated and observed hydraulic head fluctuation at three well locations.

As discussed in the following section on sensitivity analysis, there were tradeoffs in the ability to match all of the calibration objectives. For example, improved match to observed spring discharge could be attained at the expense of a degraded match to hydraulic head observations. Thus, it was not possible to quantitatively determine a "best" calibration. Rather, the resulting calibrated parameter set is based on judgment following a process that considered on the order of a hundred different trial-and-error parameter combinations.

Figure 11 shows a comparison of simulated and observed spring discharge measurements for Barton Springs for the 10-year calibration period. In general, the simulated discharge follows the pattern of observations, but the response to individual recharge events tends to be "flashy," often overshooting the observed response on the rising limb, and then quickly dropping back below the observed discharge rate before the next recharge event occurs but on average following the overall trend of observations. The peak discharge rates could be better matched by reducing the value of the precipitation limit in the recharge algorithm, but doing so results in underestimation of low spring flows and cumulative spring flow. The springflow response shown in Figure 11 is the best calibration obtained from a trial-and error process that evaluated results for dozens of different combinations of recharge parameter values. Of note is that the calibrated model does a good job of matching the lowest spring discharge observations at 1 year, 5.7 years, and 7.5 years. Total cumulative discharge simulated for Barton Springs at the end of the 10-year simulation period is 463,000 acre-feet, which is within 1 percent of the observed cumulative discharge, as shown in Figure 12. The simulated 10-year cumulative spring discharge for Cold Springs is 39,000 acre-feet, which is about 7.7 percent of the total simulated spring discharge.

Figure 13 shows comparisons of simulated and observed hydraulic head values for the three observation well locations in the diffuse system. The model overestimates the hydraulic head response well 58-58-101 to a series of large recharge events between 2.5 and 5 years, but provides a reasonably good match for the remainder of the simulation period. Conversely, the simulated hydraulic head response for Well 58-50-301 matches

the pattern of observations but underestimates the amplitude of response. For Well 58-50-801, the simulated hydraulic head response matches observations quite well.

The calibrated values for conduit- and diffuse-system storage parameters are listed in Table 3. The calibrated values for the precipitation-to-recharge algorithm parameters and a plot of the resulting transfer function are shown in Figure 14. This transfer function shows the average monthly recharge applied to the model area as a function of monthly precipitation

Table 3. Calibrated storage parameter values for transient simulation

Parameter	Value
Conduit Specific Yield	0.0004
Conduit Specific Storage	0.000001 ft^{-1}
Diffuse System Specific Yield	0.003
Diffuse System Specific Storage	0.000005 ft^{-1}

9.2 Sensitivity Analysis

The specific yield and specific storage parameters were important to the model's ability to match hydraulic head fluctuations in the three observation wells. During the calibration process, attempts were made to attenuate the flashy response of the simulated spring discharge by increasing the values of these storage parameters. Increasing the aquifer storage capacity has the effect of reducing the amplitude and spreading out the time response of discharge peaks. Although the increased aquifer storage capacity had the desired effect of damping the spring-discharge response, it also had the undesired effect of nearly eliminating the hydraulic-head response at all three observation wells. For this reason, the calibrated values for the storage parameters reflect the highest values that could be assigned without significantly degrading the modeled response to hydraulic heads in the observation wells.

As previously mentioned, the calibrated transient model used the base case steady-state model (Calibration 1), which assigns a value of 0.001 per day to the conduit-diffuse exchange parameter. To evaluate sensitivity of the transient model to the conduit-diffuse exchange parameter, the calibrated transient model results are compared to results obtained from the alternative steady-state model (Calibration 2), which assigns a value of 0.01 per day to the conduit-diffuse exchange parameter. A comparison of simulated and observed spring discharge rates for the alternative model is shown in Figure 15. Compared to the base case calibrated model (Figure 11), the alternative model slightly reduces the simulated discharge peaks immediately following recharge events by permitting faster movement of water from conduits into the diffuse flow system. However, the alternative model does not do as well in matching the low spring discharge rates at 1 year, 5.7 years, and 7.5 years. This alternative model also had the effect of slightly increasing the amplitude of response for the simulated hydraulic heads at the three observation well locations. Given the relatively low sensitivity of the model results to the diffuse-conduit exchange rate, precise knowledge of this parameter value is not considered critical to the predictive ability of the model. Overall, the base case model is

considered a better match to observations because of the priority placed on reproducing low springflow conditions.

Sensitivity to the proportion of focused versus distributed recharge fraction was also assessed. Figure 16 shows spring discharge results for a model in which the proportion of focused recharge was decreased from 85 percent to 70 percent with a corresponding increase in distributed recharge. These results are similar to the base case transient model, but the model does not match the low springflow conditions at 7.5 years quite as well. Additionally, the increased fraction of distributed recharge caused the hydraulic heads in the northern parts of the recharge area to increase significantly, which suggests a need to recalibrate steady-state conditions to the revised recharge distribution. Overall, the modeled spring discharge response does not appear to be very sensitive to the distribution of focused versus distributed recharge for the range considered.

Sensitivity to drain conductance was also evaluated to determine whether some form of resistance to flow near the spring discharge locations might attenuate the rapidity of spring response to recharge events. Reducing drain conductance by 50 percent had little effect on the spring discharge response but resulted in elevated water levels throughout the model domain that did not match observations. The spring discharge is relatively unaffected by reduced drain conductance because the hydraulic gradient across the drain cells increases in proportion to the reduction in conductance.

10 Water Budget

Water budget summaries for the steady-state simulation and for three time periods during the transient simulation are provided in Table 4. Note that, although the steady-state model is calibrated to reproduce average water level conditions measured during the time period of July–August, 1999, the computed volumes in the water budget for the steady-state model should not be construed to represent recharge or discharge volumes for this period. As with all MODFLOW-based models, the steady-state simulation consists of a single time step with duration of one time unit (1 day in this case). The steady-state water budget information, therefore, is useful only to demonstrate that mass balance is achieved in the simulation and that the input recharge and well pumping rates are as specified in the input. As indicated in Table 4, the cumulative error in water balance (i.e., difference between simulated inflows and outflows) was zero for the Calibration 1 and Calibration 2 steady-state models, and the one-day recharge, pumping, and discharge volumes are consistent with the specified input rates.

Unlike the steady-state simulation, the water budget for the transient simulation does represent an estimate of water volumes moving into and out of the aquifer during the simulation period. The transient water budget information is useful for understanding how the aquifer storage volume and spring discharge respond to varying recharge inflow and well-pumping demands. To illustrate these aquifer responses, Figure 17 shows plotted values for the simulated net volumes of recharge, well pumping, springflow, and change in storage for each monthly time step. The monthly recharge input is specified as a function of monthly precipitation (Figure 10) using the recharge algorithm described in

Section 7. The specified well-pumping demand can be seen to vary seasonally, with highest demand during the summer months, and a gradual increase in annual average pumping demand over the 10-year simulation period. Overall, well pumping constitutes about 6 percent of the total water budget for this period. Springflow and aquifer storage volume can be seen to respond strongly to recharge.

Since the vast majority of aquifer storage capacity lies within the diffuse system, and 85 percent of recharge and 94 percent of the discharge occurs through the conduit system, an approximation of the volume exchanged between the conduits and the diffuse system is gained by examining the change-in-storage volumes for each time step in the transient simulation, shown in the new Figure 17. Negative change-in-storage in excess of the well pumping rate for a given stress period generally indicates periods with low recharge when water is moving from the diffuse systems to the conduit system. Positive change-in-storage that exceeds the 15 percent of recharge assigned to the diffuse system generally indicates high-recharge periods with flow from conduits into the diffuse system.

Approximately 52 percent of total recharge in the transient simulation was applied to the outcrop area within Hays County and the remaining 48 percent was applied to outcrop area in Travis County. As indicated in Table 4, well pumping utilized approximately 6 percent of the total recharge during the transient simulation period. Approximately two-thirds of that pumping was withdrawn in Hays County with the remaining third from Travis County. All spring discharge occurs in Travis County.

Table 4. Water budget summary

	Steady-State	Transient December 31, 1994	Transient December 31, 1996	Transient December 31, 1998
Cumulative Recharge (acre-ft)	**119**	**345,342**	**433,443**	**572,337**
Cumulative Well Pumping (acre-ft)	**10.2**	**20,170**	**28,160**	**36,759**
Cumulative Springflow (acre-ft)	**108.8**	**289,950**	**379,036**	**492,910**
Cumulative Storage change (acre-ft)	**0.0**	**35,222**	**26,247**	**42,669**
Cumulative Error Inflow–Outflow (acre-ft)	**0.0**	**0.6**	**0.8**	**0.9**
Cumulative Error (percent of inflow)	**0.0**	**0.00017%**	**0.00019%**	**0.00016%**

11 Limitations of the Model

As seen in the transient simulations, the model is limited in its ability to precisely match the magnitude and response time of spring discharge peaks following precipitation events. In general the model matches well the timing of the initial increase in spring flow in response to precipitation events, but tends to behave in a "flashy" manner by overshooting some of the predicted peak discharges and also predicting a more rapid drop from the peak discharge than is observed for most events.

A potential explanation for the difficulty in matching the springflow peaks is a secondary water storage mechanism outside of the modeled aquifer domain that results in a delay between the time of precipitation and the time of recharge. For example, if the amount that the model overshoots in predicted discharge was to be held in storage and released gradually, the match to time-varying spring discharge could be much improved. A physically based and plausible mechanism for such behavior is vadose zone storage in which a portion of infiltrating water is delayed by slow drainage through soil and lateral flow from the contributing zones to recharge zones. This type of response could easily be incorporated into the conceptual model through use of a more complex precipitation-to-recharge algorithm that accounts for a fraction of the recharge being delayed. Some additional research and numerical experimentation would be required to develop an enhanced recharge algorithm, but a benefit of the effort would be a better understanding of the role of vadose zone storage and its importance to making effective groundwater management decisions. Note that, because the recharge algorithm is applied entirely outside of the numerical model, improvements to the algorithm could be implemented without the need to recalibrate the model hydraulic conductivities and storage parameters.

Overall, the modeled transient well responses are improved compared to the original Groundwater Availability Model that did not include conduits. However, the model does not precisely match well responses in all areas of the model domain. Of the three observation wells considered, the model tended to overpredict the amplitude of response for one well (58-58-101); it underpredicted response amplitude for a second well (58-50-301); and was generally consistent with observations for a third well (58-50-801). Because the well responses to recharge events are quite sensitive to the aquifer storage parameters, the assumption of uniform values for specific yield and specific storage throughout the model domain limits the ability to consistently match observed head responses in all areas of the model. Assigning these storage parameters separately for each diffuse-system zone would be one way to improve the predicted well response. Predicted well responses might also be improved by additional complexity in the precipitation-to-recharge algorithm as suggested in the preceding paragraph.

12 Future Improvements and Recommendations

Based on the results of the transient simulations, it is apparent that an additional mechanism exists for storage and release of water beyond what is considered in the updated model. We propose that this storage and release mechanism can be best explained by vadose zone storage and slow release of a portion of the recharge that is not

directly recharged to the aquifer through the focused recharge locations in streambeds. In simpler terms, not all recharge reaches the aquifer during the same month that the precipitation occurred. A recommended future improvement that could be accomplished without further modification to the Groundwater Availability Model would be to account for the vadose zone storage and release through a more complex precipitation-to-recharge algorithm.

As described in this report, the approach of treating lateral model boundaries as no-flow boundaries was carried forward from previous modeling efforts. An important management objective for this model is improved ability to predict low spring flows during severe droughts, but even very small lateral boundary fluxes could affect minimum spring flow rates during periods with no other inflow to the system. Future site characterization activities focused on understanding potential boundary fluxes could, therefore, be of great benefit to the ability to predict low spring flows. A recommended area of focus in this regard is the southwest model boundary that is intended to represent a fixed groundwater divide in the vicinity of the Blanco River south of Buda. During times of drought over the model area, it is possible that the groundwater divide could shift southward, resulting in net lateral inflow across the southwest model boundary. This process could reverse during periods of high recharge, resulting in net outflow across the model boundary. If such a process is identified, it could easily be incorporated into the model using the MODFLOW General Head Boundary package to simulate time-varying boundary conditions in that region of the model. Future modeling work could focus on evaluating the sensitivity of the model to time-varying boundary conditions as a way to help establish goals for such characterization work.

With the explicit consideration of a conduit flow system to the model, groundwater managers may wish to assess the model's ability to predict groundwater travel times from various points in the system to spring discharge or well pumping locations. The MODPATH particle-tracking algorithm could be used in conjunction with the updated model to evaluate the ability of model to predict tracer travel times in conduits.

MODFLOW–DCM Version 2.0 does not include a graphical user interface. The processing and graphical display of data and model results for this study was accomplished with Mathematica Version 5.2 (Wolfram Research, Inc., 2005). Wolfram Research, Inc, recently developed Mathematica Version 7.0, which has the capability to create data processing and visualization utilities that can be utilized with low-cost or free "Player" versions of their software. The utilities used for processing information in this study could easily be upgraded to Mathematica Version 7 and provided to Barton Springs Edwards Aquifer Conservation District and TWDB staff for use as a graphical postprocessor without the need to buy a full Mathematica license.

13 Conclusions

The Groundwater Availability Model for the Barton Springs segment of the Edwards (Balcones Fault Zone) Aquifer was updated by extending the model domain to the south and west and by modifying the model to explicitly include a network of conduits within

the aquifer body. This updated model is designed to be run using MODFLOW–DCM Version 2.0 (Painter and others, 2007). The model updates necessitated recalibration for steady-state and transient conditions. In addition to the model updates and calibrations, an initial algorithm was developed for estimating recharge input to the model based on average monthly precipitation over the recharge and contributing zones. The root-mean-square residual error for the updated steady-state model is reduced to approximately half that of the original Groundwater Availability Model. The transient model was able to reproduce the pattern of hydraulic head fluctuations in observation wells, and observed discharge at Barton Springs using recharge input that was developed from the precipitation-to-recharge algorithm. The calibrated transient model generally matched patterns of observed springflow and the cumulative spring flow for the 10-year simulation period. Development of a more complex precipitation-to-recharge algorithm is recommended to account for a portion of recharge that can be delayed by slow drainage from the vadose zone.

14 Acknowledgments

This study was jointly funded by the Barton Springs Edwards Aquifer Conservation District and the Texas Water Development Board (TWDB). The authors gratefully acknowledge the technical guidance, direction, and access to data provided by Dr. Brian Smith of Barton Springs Edwards Aquifer Conservation District and Dr. Ian Jones of the TWDB.

This report is an independent product of the Geosciences and Engineering Division of Southwest Research Institute® and does not necessarily reflect the views or positions of the funding organizations. The authors wish to thank the following Geosciences and Engineering Division staff members for their contributions: Drs. Gary Walter and David Ferrill for their technical and programmatic review comments; Ms. Cheryl Patton for formatting and technical editing of the report. The authors also are grateful to Ms. Kate Walker for her assistance with input data reduction and development of data processing utilities.

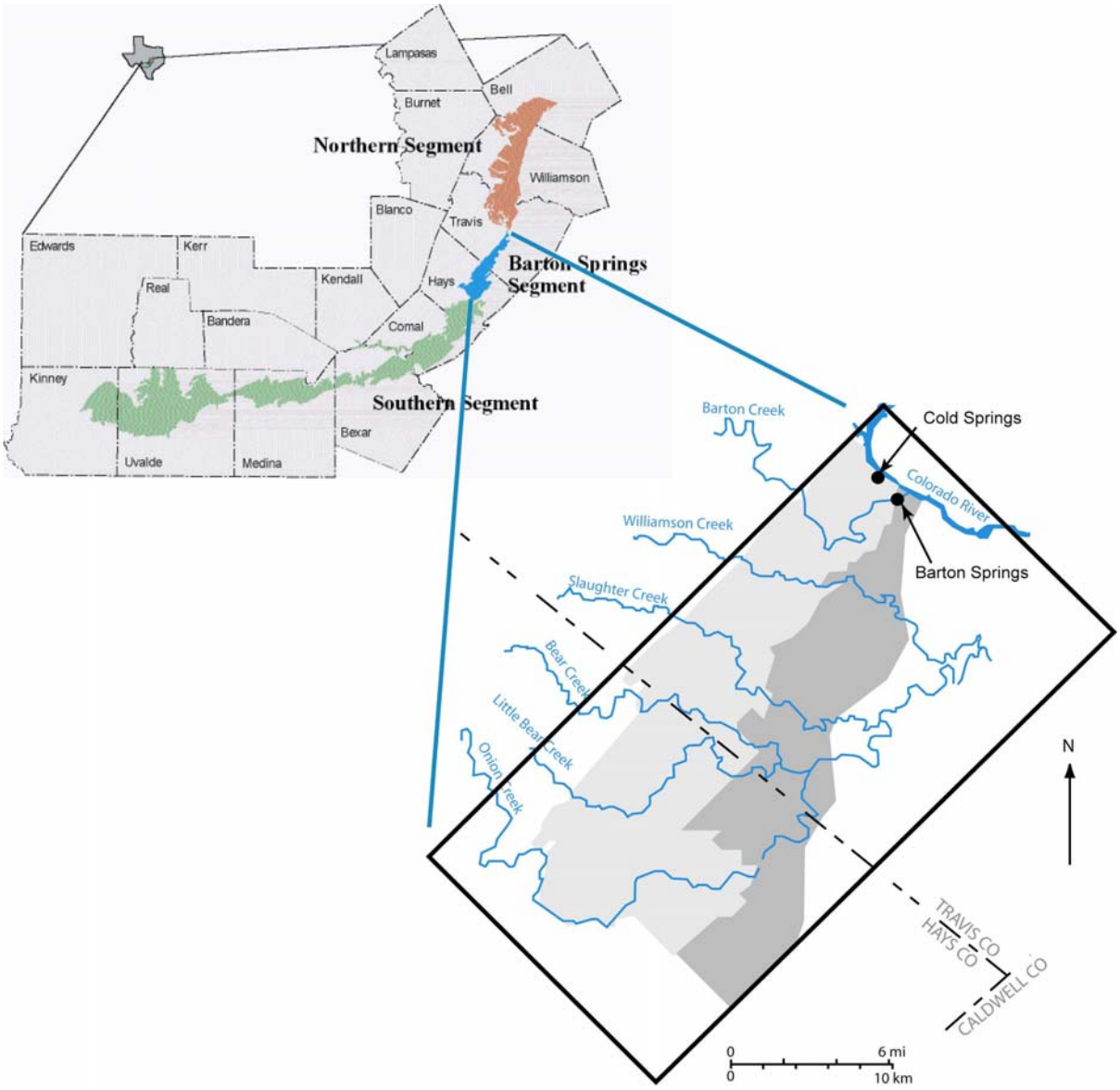

Figure 1. Study area for the Barton Springs model. The model domain is indicated by the black box. Light and dark gray shaded areas indicate unconfined and confined zones in the original Groundwater Availability Model by Scanlon and others (2001). Watersheds northeast of the unconfined outcrop area constitute the contributing zone.

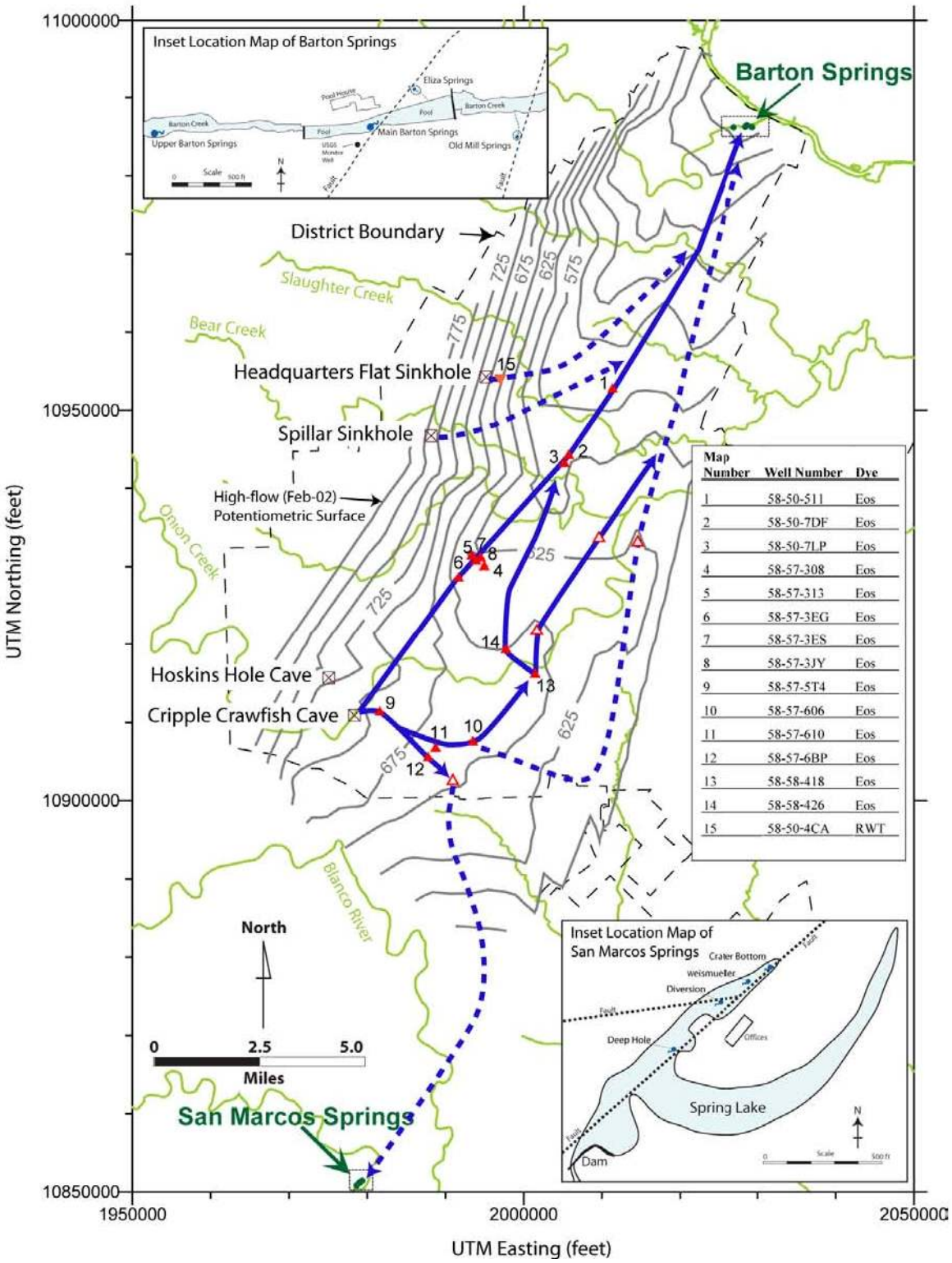

Figure 2. Conduit locations, inferred from tracer test results (from Hunt and others, 2006) are shown as solid and dashed blue lines.

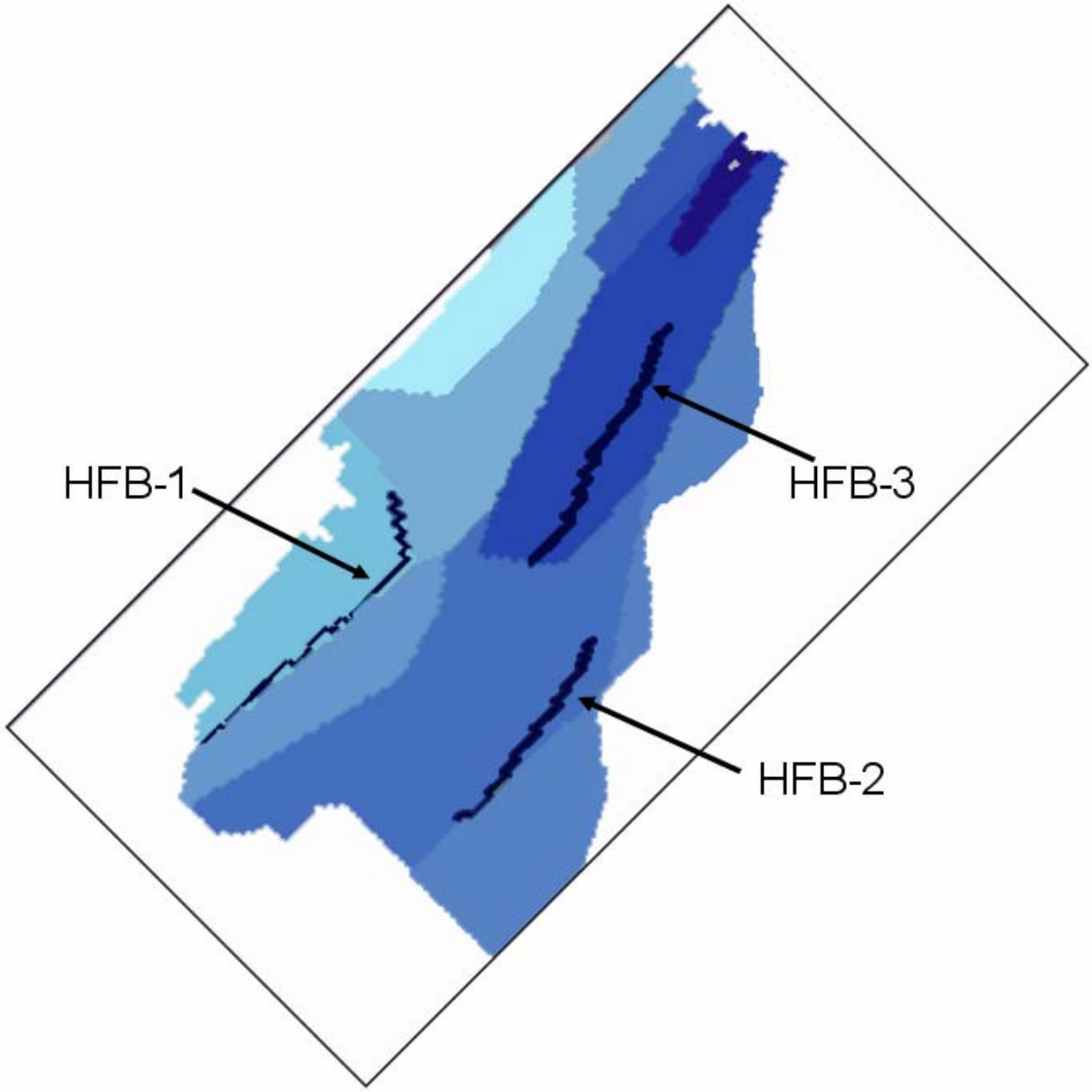

Figure 3. Locations of three horizontal flow barriers assigned to the Groundwater Availability Model by Scanlon and others (2001), which were retained for this study. The black border indicates the same model domain as shown in Figure 3.

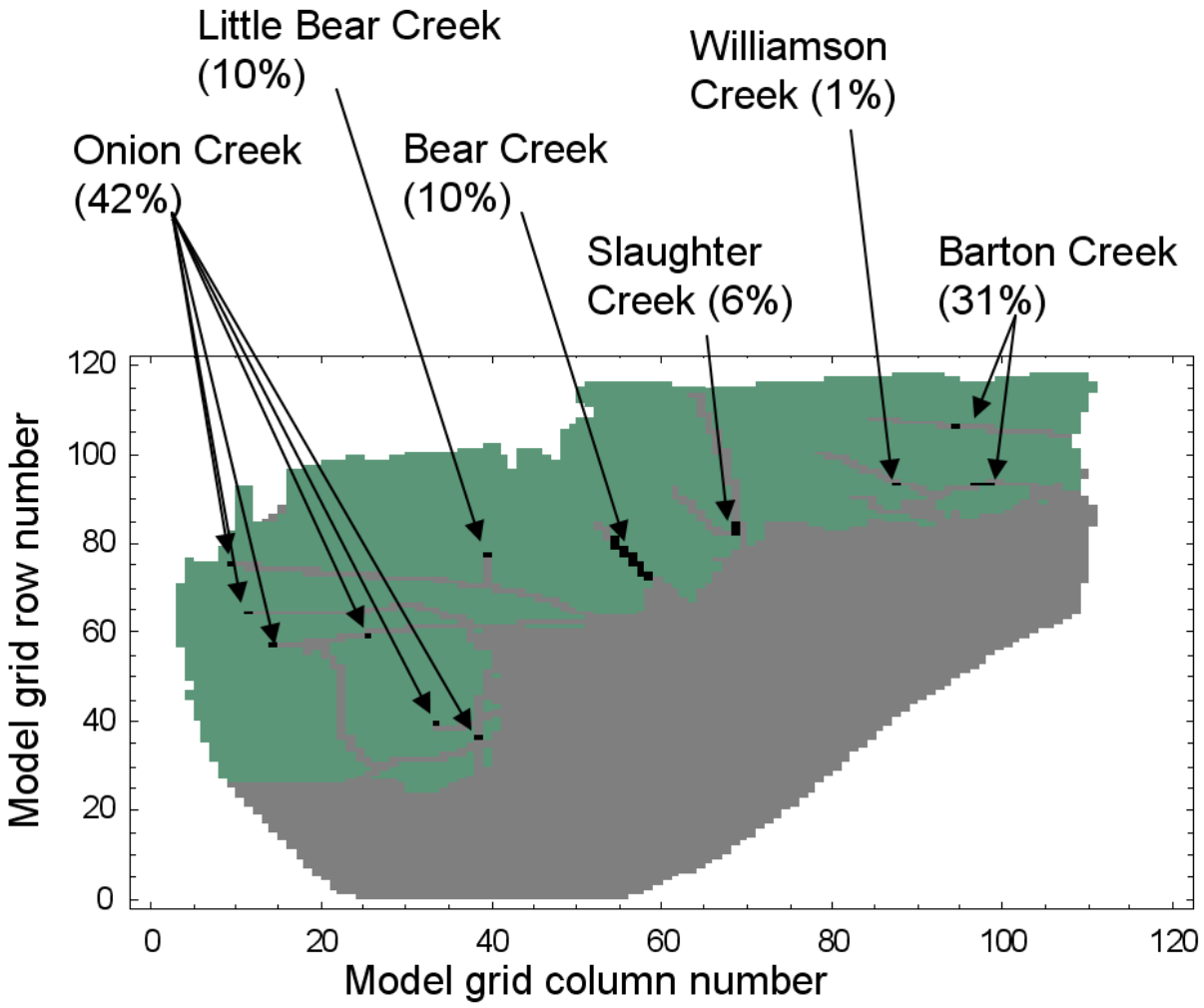

Figure 4. Focused recharge locations. Percentages indicate approximate fraction of focused recharge (85 percent of total recharge) apportioned to each recharge feature. For features with more than one recharge cell location, the amount of recharge to that feature is evenly divided among the cells. Diffuse recharge is assumed to be 15 percent of total recharge and is evenly distributed across the green-shaded cells.

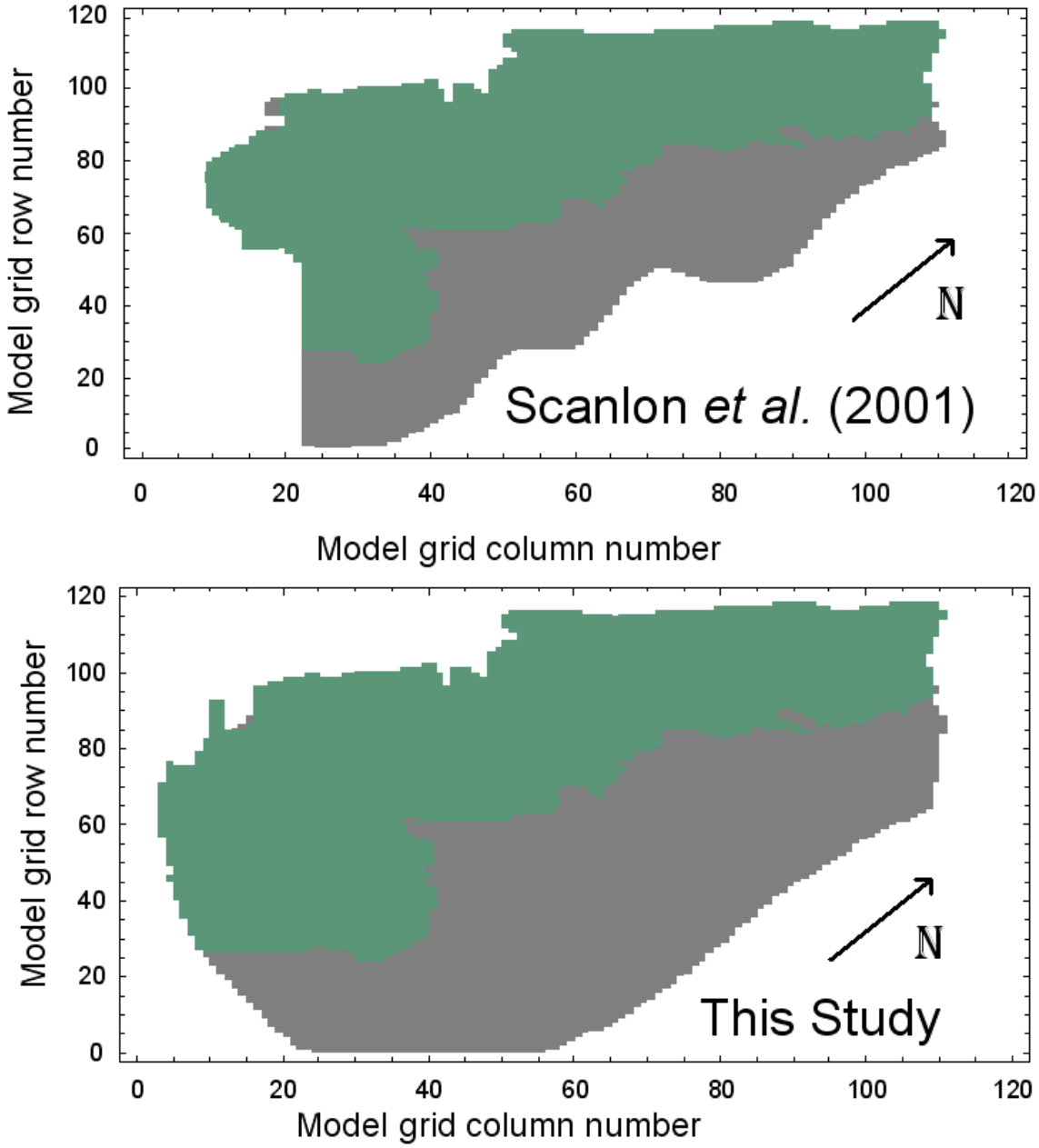

Figure 5. Comparison of the active model domains (green and gray shaded areas) for the Scanlon and others (2001) model and the model used in this study. The green shaded area indicates the recharge zone where the Edwards formation is present in outcrop.

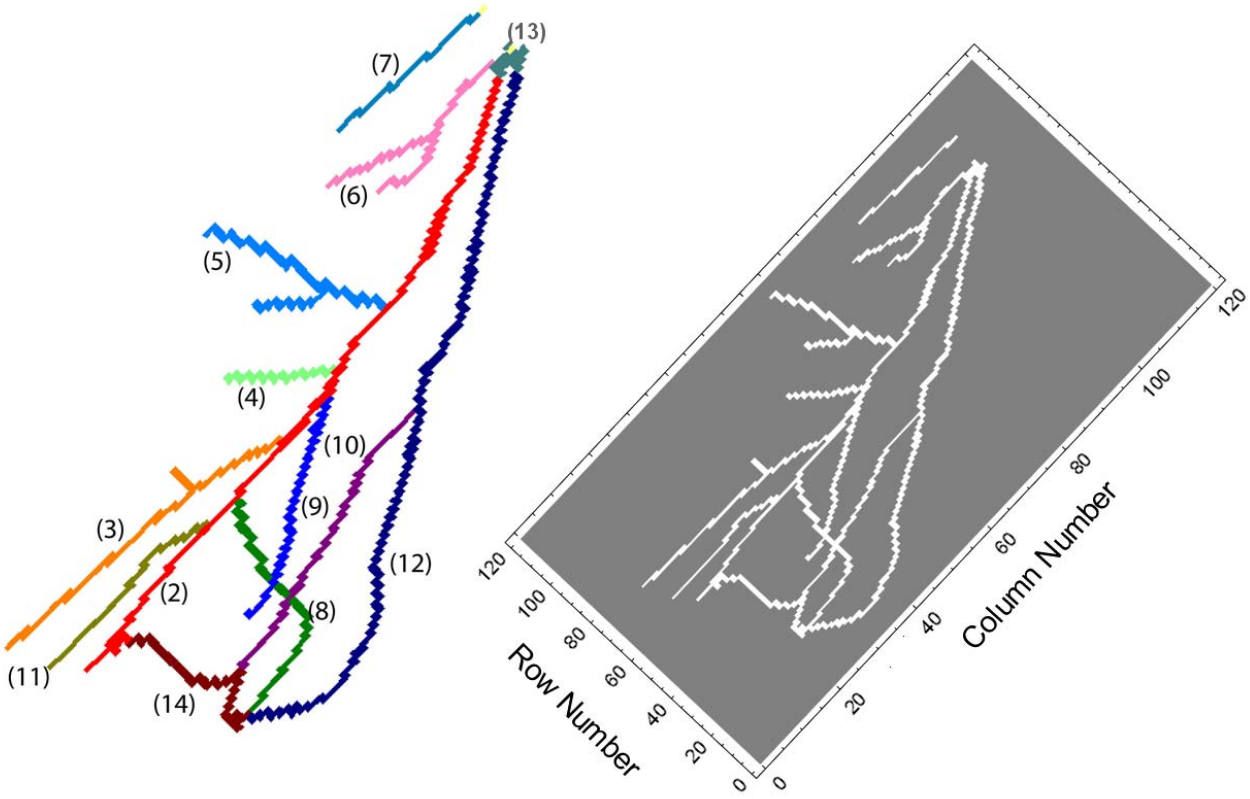

Figure 6. Conduit designations (left) and locations within the model domain (right). Rows and columns designate model cells with dimensions 500 ft wide by 1000 ft long. Cells in gray shaded area are treated as inactive.

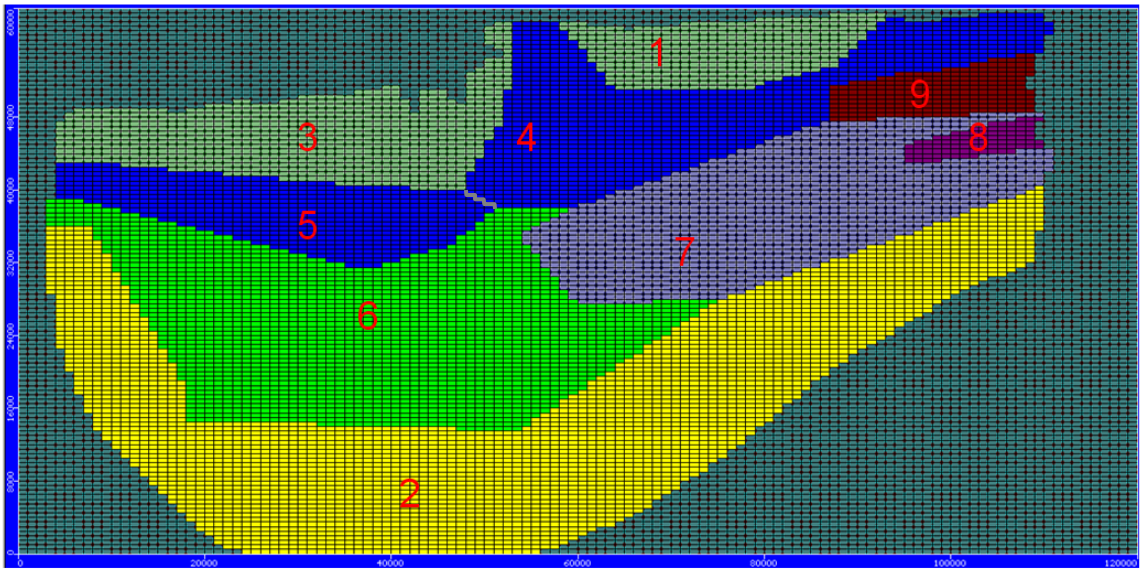

Figure 7. Model grid showing nine diffuse-system hydraulic conductivity zones used in the steady-state calibration.

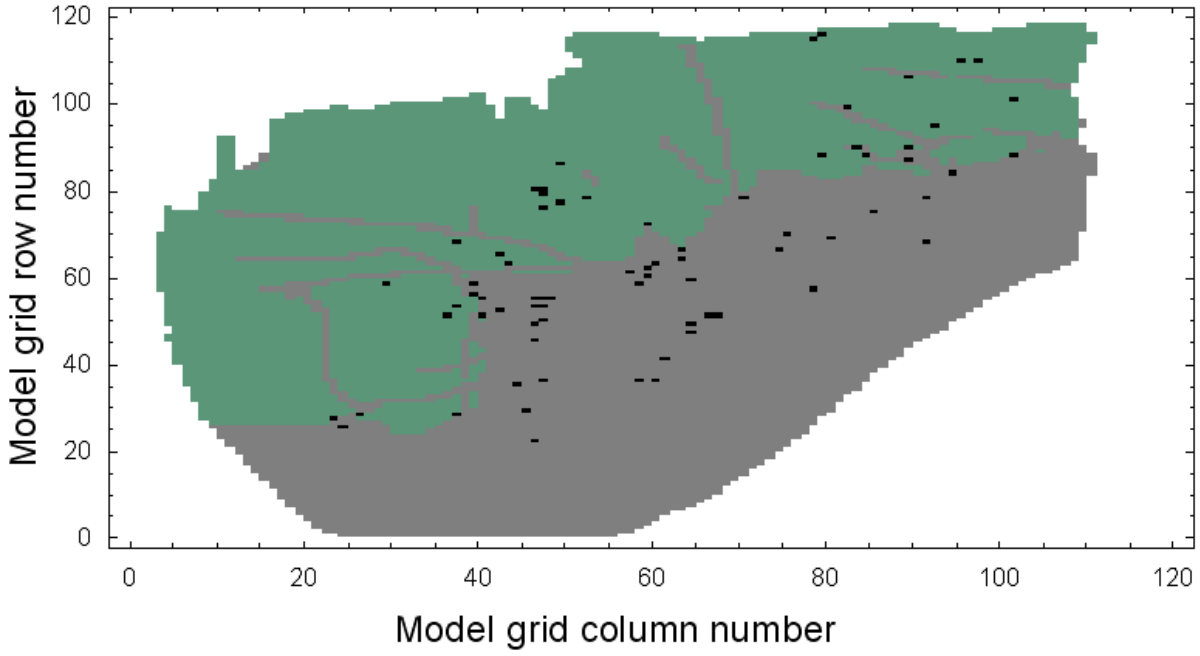

Figure 8. Locations of observation wells used in the steady-state calibration.

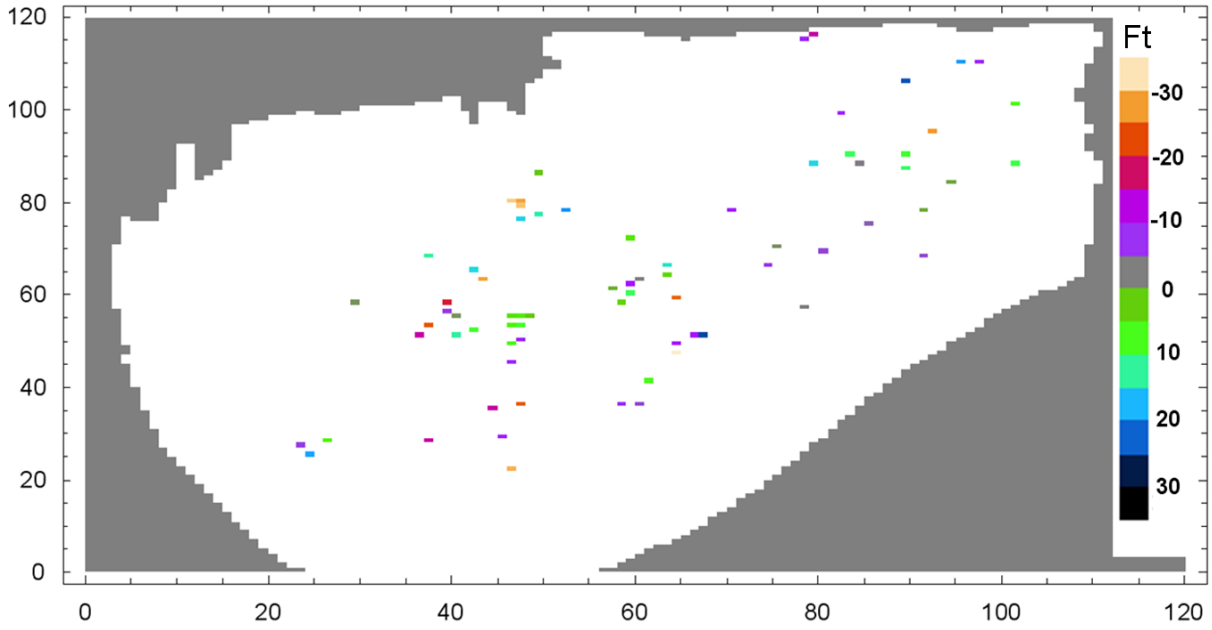

Figure 9. Spatial distribution of steady-state calibration error for Calibration 1 shows positive (cool colors) and negative (warm colors) errors are evenly distributed throughout the model domain with no significant spatial bias.

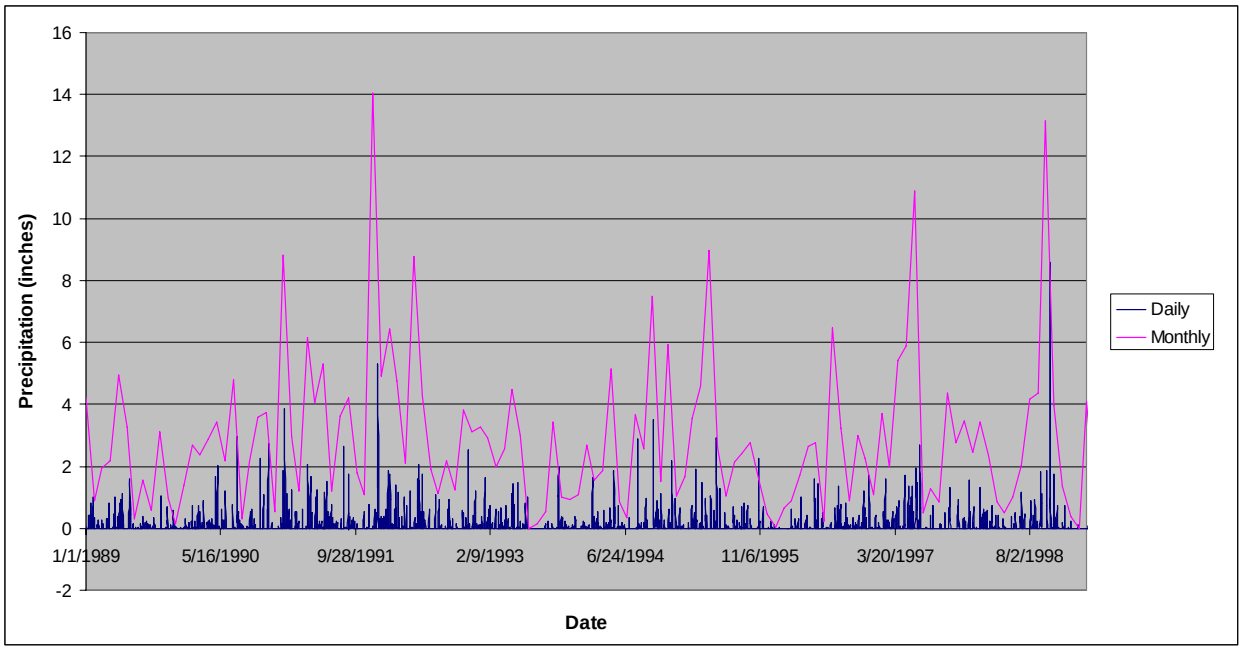

Figure 10. Precipitation record used to develop recharge input for the transient simulations.

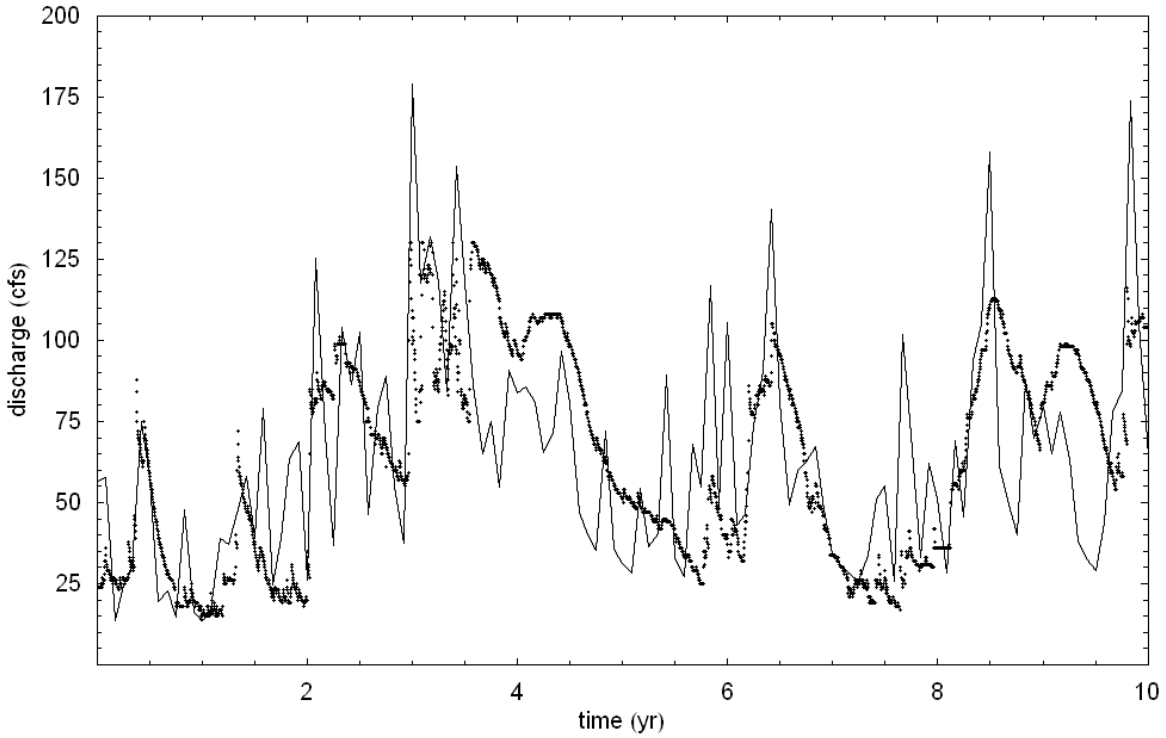

Figure 11. Simulated (line) and observed (dots) spring discharge for the 10-year transient calibration period.

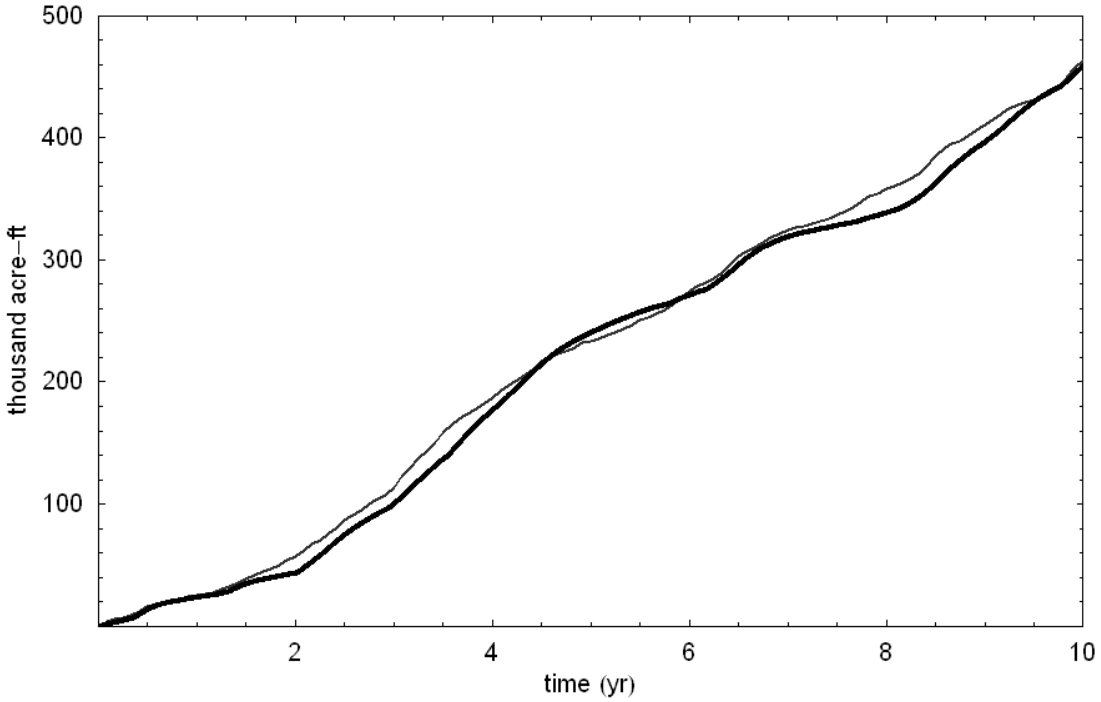

Figure 12. Simulated (thin line) and observed (thick line) cumulative spring discharge for the 10-year transient calibration period.

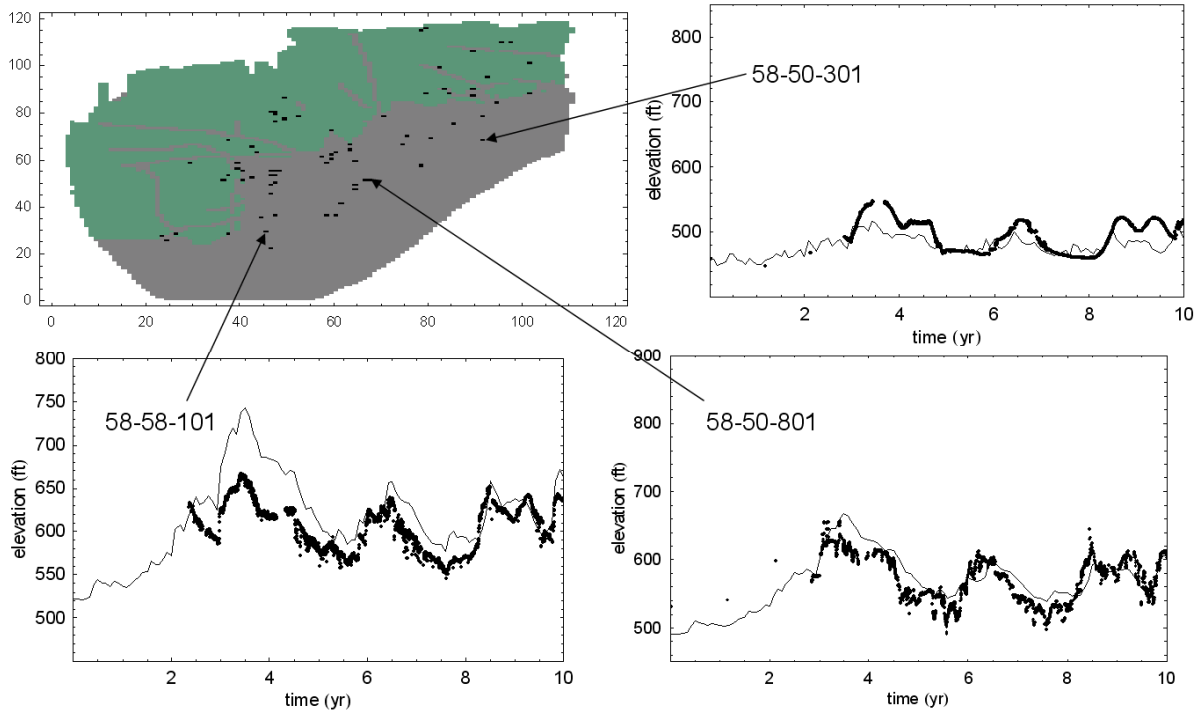

Figure 13. Comparison between simulated (lines) and observed (dots) hydraulic heads for three observation wells used in the transient model calibration.

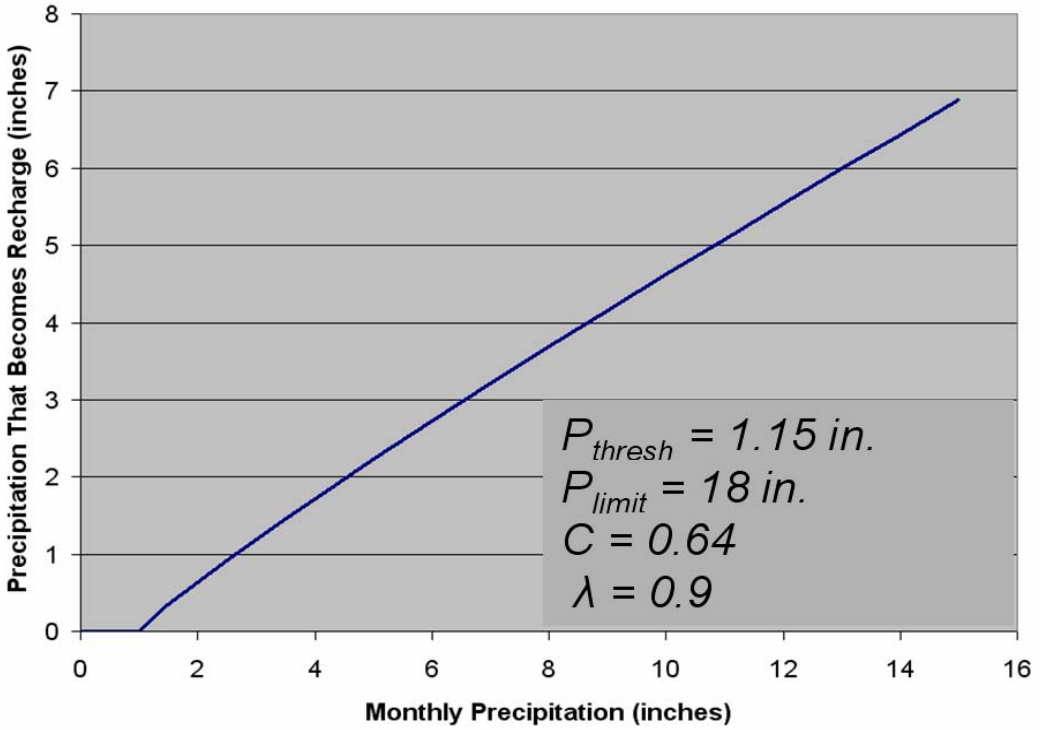

Figure 14. Calibrated parameter values and transfer function for converting average monthly precipitation to total recharge input for each monthly stress period.

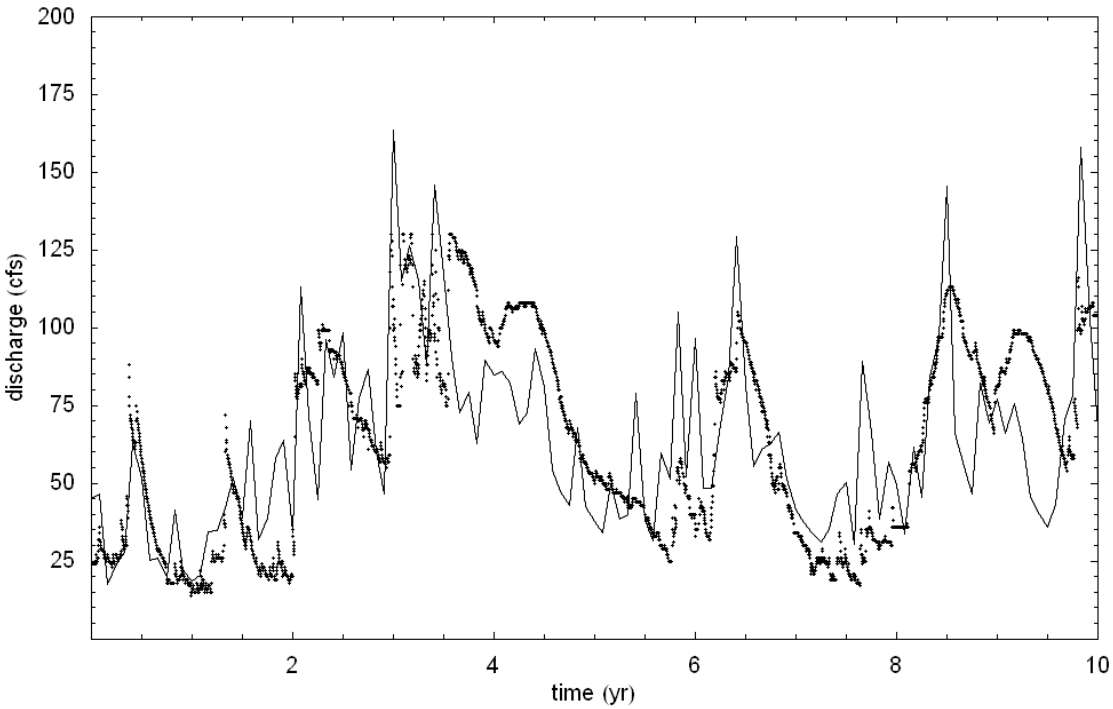

Figure 15. Simulated (line) and observed (dots) spring discharge for an alternative transient model with conduit-diffuse exchange parameter increased from 0.001per day to 0.01per day.

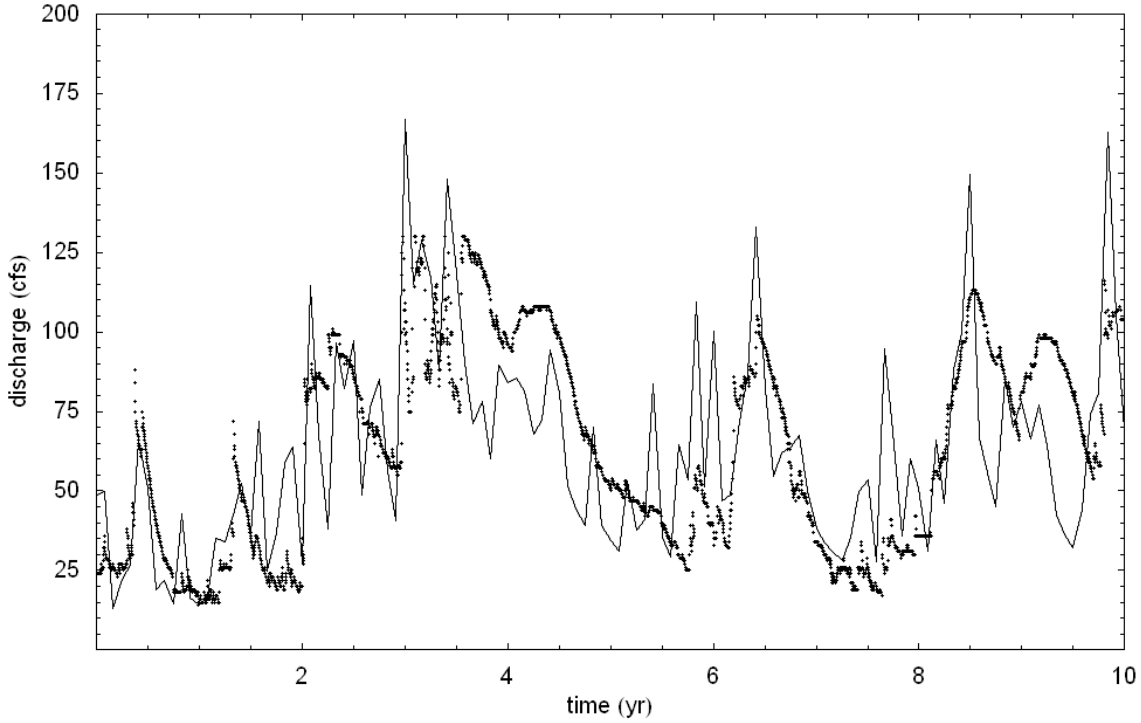

Figure 16. Simulated (line) and observed (dots) spring discharge for a transient simulation with base case parameter values and focused recharge reduced from 85 percent to 70 percent of total recharge.

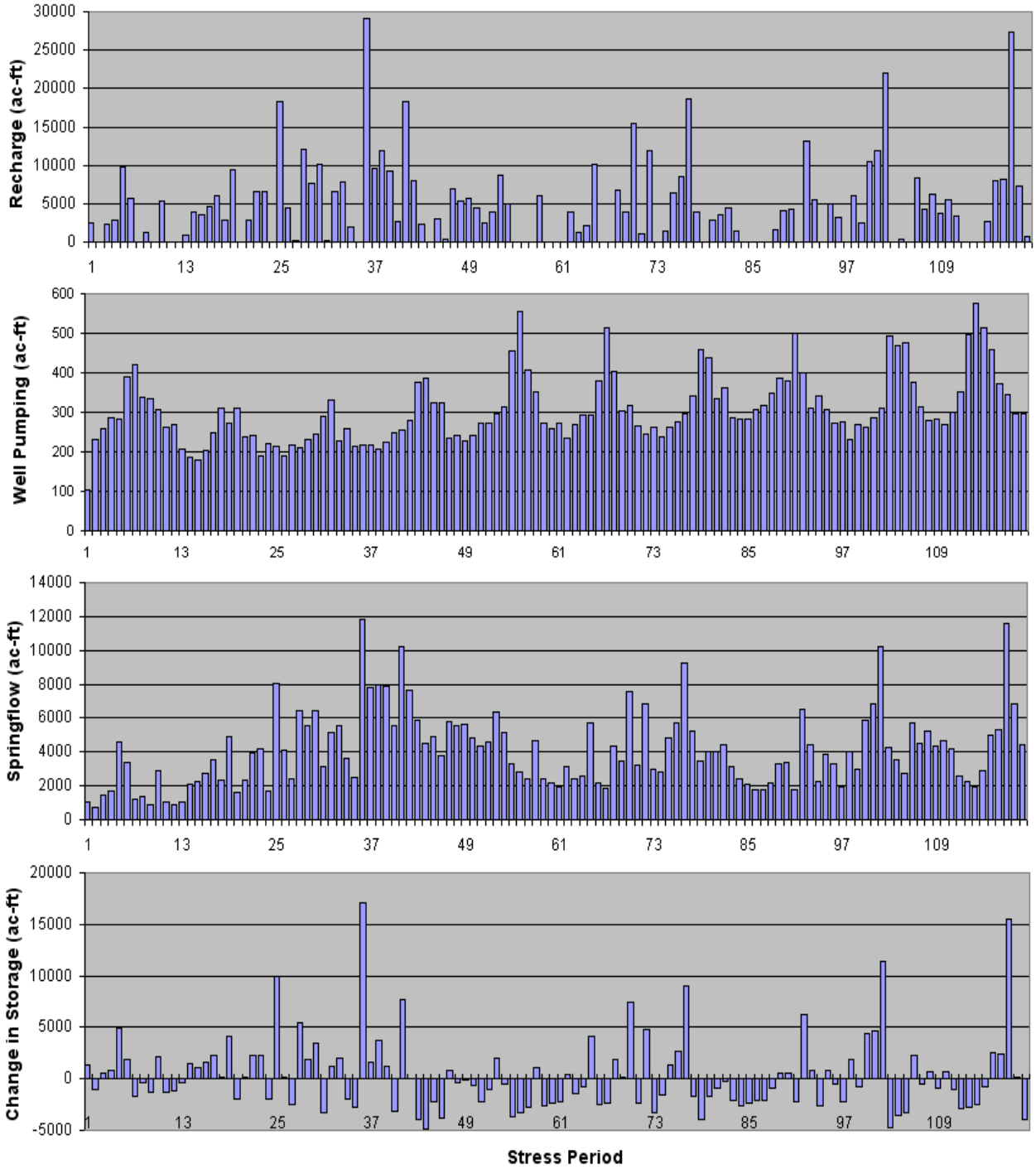

Figure 17. Water budget output data for each of the 120 monthly stress periods in the calibrated transient simulation.

14 References

Barrett, M. E., and Charbeneau, R. J., 1996. *A parsimonious model for simulation of flow and transport in a karst aquifer*. Center for Research in Water Resources, Report No. 269, 149 p.

Hauwert, N.M, D.A. Johns, J.W. Sansom, and T.J. Aley. 2002. *Groundwater tracking of the Barton Springs Edwards Aquifer, Travis and Hays Counties, Texas*. Gulf Coast Association of Geological Societies Transactions 52. pp. 377–384.

Hunt, B.B., B.A. Smith, J. Beery, D. Johns, and N. Hauwert. 2006. *Summary of 2005 Groundwater Dye Tracing, Barton Springs Segment of the Edwards Aquifer, Hays and Travis Counties, Central Texas*. BSEACD Report of Investigations 2006-0530. Barton Springs/Edwards Aquifer Conservation District. Austin, Texas.

Harbaugh, A.W. and M.G. McDonald. 1996. *User's Documentation for MODFLOW–96, An Update to the U.S. Geological Survey Modular Finite-Difference Ground Water Flow Model*. U.S. Geological Survey Open File Report 96–485.

Harbaugh, A.W. E.R. Banta, M.C. Hill, and M.G. McDonald. 2000. *MODFLOW–2000, the U.S. Geological Survey Modular Ground-Water Model–User Guide to Modularization Concepts and the Ground-Water Flow Process*. U.S. Geological Survey Open File Report 00–92.

Painter, S.L., A. Sun, and R.T. Green. 2007. *Enhanced Characterization and Representation of Flow through Karst Aquifers—Phase II*. Revision 1. Geosciences and Engineering Division, Southwest Research Institute, San Antonio, TX.

Painter, S.L., H. Basagaoglu, and A. Liu. 2008. Robust Representation of Dry Cells in Single-Layer MODFLOW Models. *Ground Water, 46*(6): 873–881.

Puente, C. 1976. *Statistical analysis of water-level, springflow, and streamflow data for the Edwards Aquifer in south-central Texas*. U.S. Geological Survey Report. 58 p.

Puente, C. 1978. *Method of estimating natural recharge to the Edwards Aquifer in the San Antonio area, Texas*. U.S. Geological Survey Water Resources Investigations Report 78–10. 34 p.

Scanlon, B.R., R.E. Mace, B. Smith, S. Hovorka, A.R. Dutton, and R. Reedy. 2001. *Groundwater Availability Modeling of the Barton Springs Segment of the Edwards Aquifer, Texas: Numerical Simulations Through 2050.* Austin, Texas. Bureau of Economic Geology.

Slade, R. M., Ruiz, L., and others. 1985. *Simulation of the flow system of Barton Springs and associated Edwards aquifer in the Austin area, Texas*. U.S. Geological Survey, Water Resources Investigations Report 85–4299, 49 p.

Small, T. A., J. A. Hanson, and N. M. Hauwert. 1996. *Geologic framework and hydrogeologic characteristics of the Edwards aquifer outcrop (Barton Springs segment), northeastern Hays and southwestern Travis Counties, Texas*. U.S. Geological Survey, Water-Resources Investigations WRI 96–4306, 15 p. (1 sheet).

Smith, B. and B. Hunt. 2004. *Evaluation of the sustainable yield of the Barton Springs Segment of the Edwards Aquifer, Hays and Travis Counties, Central Texas*. Barton Springs/Edwards Aquifer Conservation District. Austin, Texas.

Wolfram Research, Inc. 2005. Mathematica, Version 5.2. Champaign, IL.

APPENDIX A: INPUT INSTRUCTIONS FOR THE MODFLOW–DCM PACKAGE

A.1 Name File

To activate the DCM package, the following line needs to be added to a MODFLOW name file

DCM Nunit Fname

where Nunit is the Fortran unit to be used for file I/O and Fname is the name of the I/O file. Note that LPF, DCM, and BCF are all flow solvers and thus cannot be used simultaneously.

DCM is designed to work with a new Newton-Raphson solver NR1. The NR1 solver will be activated automatically. Other MODFLOW solvers (i.e., PCG2, GMG, DE4, SIP, etc) should not be included in the name file.

A.2 DCM Input Parameters

The structure of the DCM input file follows that of LPF. Because DCM only allows one diffuse layer and one conduit layer, vertical conductivity and vertical anisotropy parameters are not needed and are not recognized. In addition, LPF parameters related to drying and rwetting are not needed in DCM and should not be entered. DCM requires one additional global variable and two additional layer variables that are not required for LPF.

Many instructions that appear below are copied from the LPF instruction. The changes and instructions specific to DCM are highlighted in blue. Note that DCM requires input for two layers. Layer 1 represents the conduit and Layer 2 the diffuse (matrix) system.

0. [#Text]
Item 0 is optional—"#" must be in Column 1. Item 0 can be repeated multiple times.
1. ILPFCB HDRY NPDCM
2. LAYTYP(NLAY)
3. LAYAVG(NLAY)
4. CHANI(NLAY)
5. FLOWLAW
6. [PARNAM PARTYP Parval NCLU]
7. [Layer Mltarr Zonarr IZ]
Each repetition of Item 7 is called a parameter cluster. Repeat Item 7 NCLU times. Repeat Items 6—7 for each parameter to be defined (that is, NPDCM times).

A subset of the following two-dimensional variables is used to describe each layer. All the variables that apply to Layer 1 are read first, followed by Layer 2. If a variable is not required due to simulation options (for example, SS and SY for a completely steady-state simulation), then it must be omitted from the input file.

These variables are either read by the array-reading utility module, U2DREL, or they are defined through parameters. If a variable is defined through parameters, then the variable itself is not read; however, a single record containing a print code is read in place of the array control record. The print code determines the format for printing the values of the variable as defined by parameters. The print codes are the same as those used in an array control record. If any parameters of a given type are used, parameters must be used to define the corresponding variable for all layers in the model.

8. HK(NCOL,NROW) If there are any HK parameters, read only a print code.

9. [HANI(NCOL,NROW)] Include Item 9 only if CHANI is less than or equal to 0. If there are any HANI parameters, read only a print code.

10. [CRTG(NCOL,NROW)] Include Item 10 only for Layer 1 when FLOWLAW is equal to 1. If there are no CRTG parameters, read only a print code.

11 [SS(NCOL,NROW)] Include Item 11 only if at least one stress period is transient. If there are any SS parameters, read only a print code.

12. [SY(NCOL,NROW)] Include Item 12 only if at least one stress period is transient and LAYTYP is not 0. If there are any SY parameters, read only a print code.

13. CDEX(NCOL,NROW) Read Item 13 only for Layer 1. If there are any CDEX parameters, read only a print code.

ILPFCB – is a flag and a unit number.
If ILPFCB > 0, it is the unit number to which cell-by-cell flow terms will be written when "SAVE BUDGET" or a nonzero value for ICBCFL is specified in Output Control. The terms that are saved are storage, constant-head flow, and flow between adjacent cells.
If ILPFCB = 0, cell-by-cell flow terms will not be written.
If ILPFCB < 0, cell-by-cell flow for constant-head cells will be written in the listing file when "SAVE BUDGET" or a nonzero value for ICBCFL is specified in Output Control. Cell-by-cell flow to storage and between adjacent cells will not be written to any file.

HDRY – is not used in DCM, but should be present in the input.

NPDCM – is the number of parameters.

LAYTYP – indicates the layer type. Enter one value for each layer. Value 0 represents confined layer type, and nonzero value represents unconfined layer type.

LAYAVG – indicates the method for calculating intercell conductances. One value is needed for each layer.
0 – harmonic mean
1 – logarithmic mean

For a detailed description of the averaging methods, please refer to the User's Manual for MODFLOW2000. In DCM, these averaging methods apply only to the hydraulic conductivity. Upstream weighting of the saturated thickness is used in DCM to calculate the intercell conductances.

CHANI – contains a value for each layer that is a flag or the horizontal anisotropy. If CHANI is less than or equal to 0, then variable HANI defines horizontal anisotropy. If CHANI is greater than 0, then CHANI is the horizontal anisotropy for the entire layer, and HANI is not read. If any HANI parameters are used, CHANI for all layers must be less than or equal to 0.

FLOWLAW – indicates the governing flow equation for conduits. Enter 0 for laminar flow (Darcy's equation) and 1 for turbulent flow (Darcy-Weisbach equation). The diffuse system is always modeled with Darcy's equation.

PARNAM – is the name of a parameter to be defined. This name can consist of 1 to 10 characters and is not case sensitive. That is, any combination of the same characters with different case will be equivalent.

PARTYP – is the type of parameter to be defined. For the DCM Package, the allowed parameter types are

HK – defines variable HK, horizontal hydraulic conductivity
HANI – defines variable HANI, horizontal anisotropy
SS – defines variable Ss, the specific storage
SY – defines variable Sy, the specific yield
CDEX – defines variable α, the linear exchange term between the conduit layer and the diffuse matrix layer. Enter for Layer 1.
CRTG – defines the critical gradient for the onset of turbulent flow in the conduit. Enter for Layer 1 if the turbulent flow law is chosen.

PARVAL – is the parameter value.

NCLU – is the number of clusters required to define the parameter. Each repetition of Item 7 is a cluster (variables Layer, Mltarr, Zonarr, and IZ). There is usually only one cluster for each layer that is associated with a parameter.

LAYER – is the layer number to which a cluster definition applies.

MLTARR – is the name of the multiplier array to be used to define variable values that are associated with a parameter. The name "NONE" means that there is no multiplier array, and the variable values will be set equal to PARVAL.

ZONARR – is the name of the zone array to be used to define the cells that are associated with a parameter. The name "ALL" means that there is no zone array, and all cells in the specified layer are part of the parameter.

IZ – is up to 10 zone numbers (separated by spaces) that define the cells that are associated with a parameter. These values are not used if ZONARR is specified as "ALL". Values can be positive or negative, but 0 is not allowed. The end of the line, a zero value, or a nonnumeric entry terminates the list of values.

HK– is the hydraulic conductivity along rows. HK is multiplied by horizontal anisotropy (see CHANI and HANI) to obtain hydraulic conductivity along columns.

HANI – is the ratio of hydraulic conductivity along columns to hydraulic conductivity along rows, where HK of Item 10 specifies the hydraulic conductivity along rows. Thus, the hydraulic conductivity along columns is the product of the values in HK and HANI. Read only if CHANI is not equal to 0.

CRTG – is the critical gradient for the onset of turbulence. Read only for Layer 1 and only if FLOWLAW > 1.

SS – is specific storage. Read only for a transient simulation (at least one transient stress period).

SY – is specific yield. Read only for a transient simulation (at least one transient stress period) and if the layer is convertible (LAYTYP is not 0).

CDEX – is the exchange term for flow between conduit and matrix system (α_0). Enter for Layer 1 only.

A.3 Example Input File

The following shows an example of DCM input file,
DCM File,

```
#Example1 DCM package
50   -1E+30        3            Item 1:  ILPFCB HDRY NPLPF
 0 0                            Item 2:  LAYTYP
 0 0                            Item 3:  LAYAVG
 1 1                            Item 4:  CHANI
 1                              Item 5:  FLOWLAW
HK_0 HK   1  2                  Item 6:  PARNAM PARTYP PARVAL NCLU
 1 HK1 ZHK1 999                 Item 7:  LAYER MARRAY ZARRAY [zones]
 2 HK2 ZHK2 999
SS_0 SS   1  2                  Item 6:  PARNAM PARTYP PARVAL NCLU
 1 SS1 ZSS1 999                 Item 7:  LAYER MARRAY ZARRAY [zones]
 2 SS2 ZSS2 999
CDEX_0 CDEX   1  1              Item 6:  PARNAM PARTYP PARVAL NCLU
 1 CDEX1 ZCDEX1 999             Item 7:  LAYER MARRAY ZARRAY [zones]
      31        1(20G14.0)                -1  10: HK of layer 1
      31        1(20G14.0)                -1  11: HANI of layer 1
      31        1(20G14.0)                -1  12: Ss of layer 1
      31        1(20G14.0)                -1  13: CDEX of layer 1
      31        1(20G14.0)                -1  10: HK of layer 2
      31        1(20G14.0)                -1  11: HANI of layer 2
      31        1(20G14.0)                -1  12: Ss of layer 2
```

The values of parameters are defined in the associated multiplier file and zone file, respectively.

Multipler file,

```
#Example1 Multiplier file
 5
HK1
Constant          0.50    4: HK Multiplier array for layer 1
HK2
Constant          0.10    4: HK Multiplier array for layer 2
SS1
Constant         .0005     4: Ss Multiplier array for layer 1
SS2
Constant         .0001     4: Ss Multiplier array for layer 2
CDEX1
Constant          0.0001  4: CDEX Multiplier array for layer 1
```

Zone file,

```
#Example1 Zone file
 7
ZHK1
Constant          999    HK zone array for layer 1
ZHK2
Constant          999    HK zone array for layer 2
ZSS1
Constant          999    SS zone array for layer 1
```

ZSS2
Constant 999 SS zone array for layer 2
ZSY1
Constant 999 SY zone array for layer 1
ZSY2
Constant 999 SY zone array for layer 2
ZCDEX1
Constant 999 CDEX zone array for layer 1

A.4 NR1 Solver Input

The NR1 solver input is read from a file called nr1in.dat. The file must be named nr1in.dat. If the file is not present, default values will be used for all input parameters. The NR1 input is given below.

1. ITMXO HTOL RTOL
2. ATYPE LEVEL NVECTORS DETAIL
3. ITMAXI R2TOL RXTOL SXTOL

Definitions for the input parameters follow.

ITMAX0 – is the maximum number of outer iterations.

HTOL – is the head tolerance [L] used to define convergence in the outer iterations.

RTOL – is the residual tolerance [L^3/T] used to define convergence in the outer iterations.

ATYPE – is an integer-controlling selection of accelerator in a preconditioned conjugate gradient linear solver. Currently, the only allowed value is 4, which corresponds to the bi-conjugate gradient stabilized method. Alternative values may be available in future versions.

LEVEL – is the level of infill allowed in the incomplete lower-upper decomposition used for preconditioning. Recommended values are 1 or 0.

NVECTORS – is read but not currently used.

DETAIL – is an integer controlling output from the linear solver. Enter 0 for no output, 1 for summary output, and 2 for residual information at each inner iteration. Output is written to the file NR1OUT.DAT.

ITMAXI – is the maximum number of inner iterations.

R2TOL – is a convergence criterion based on the Euclidian norm of the residual.

RXTOL – is a convergence criterion based on the maximum residual.

SXTOL – is a convergence criterion based on the maximum scaled solution update.